

## **Osteology of the alvarezsauroid *Linhenykus monodactylus* from the Upper Cretaceous Wulansuhai Formation of Inner Mongolia, China, and comments on alvarezsauroid biogeography**

Xing Xu, Paul Upchurch, Qingyu Ma, Michael Pittman, Jonah Choiniere, Corwin Sullivan, David W. E. Hone, Qingwei Tan, Lin Tan, Dong Xiao, and Fenglu Han

*Acta Palaeontologica Polonica* in press


available online 13 Dec 2011 doi: <http://dx.doi.org/10.4202/app.2011.0083>

The alvarezsauroid *Linhenykus monodactylus* from the Upper Cretaceous of Inner Mongolia, China is the first known monodactyl non-avian dinosaur, providing important information on the complex patterns of manual evolution seen in alvarezsauroids. Here we provide a detailed description of the osteology of this taxon. *Linhenykus* shows a number of features that are transitional between parvicursorine and non-parvicursorine alvarezsauroids, but detailed comparisons also reveal that some characters had a more complex distribution. We also use event-based tree-fitting to perform a quantitative analysis of alvarezsauroid biogeography incorporating several recently discovered taxa. The results suggest that there is no statistical support for previous biogeographic hypotheses that favour pure vicariance or pure dispersal scenarios as explanations for the distributions of alvarezsauroids across South America, North America and Asia. Instead, statistically significant biogeographic reconstructions suggest a dominant role for sympatric (or ‘within area’) events, combined with a mix of vicariance, dispersal and regional extinction. At present the alvarezsauroid data set is too small to completely resolve the biogeographic history of this group: future studies will need to create larger data sets that encompass additional clades.

**Key words:** Theropoda, Parvicursorinae, alvarezsauroid, biogeography, Treefitter, dispersal, vicariance, sympatry, Late Cretaceous, Wulansuhai Formation, Mongolia, China.

Xing Xu [[xingxu@vip.sina.com](mailto:xingxu@vip.sina.com)], Qingyu Ma [[maqingyu.ivpp@gmail.com](mailto:maqingyu.ivpp@gmail.com)], Corwin Sullivan [[csullivan@ivpp.ac.cn](mailto:csullivan@ivpp.ac.cn)], David W.E.Hone [[dwe\\_hone@yahoo.com](mailto:dwe_hone@yahoo.com)], and Fenglu Han [[hfl0501@gmail.com](mailto:hfl0501@gmail.com)], Key Laboratory of Evolutionary Systematics of Vertebrates, Institute of Vertebrate Paleontology & Paleoanthropology, Chinese Academy of Sciences, 142 Xiwai Street, Beijing 100044, China; Paul Upchurch [[p.upchurch@ucl.ac.uk](mailto:p.upchurch@ucl.ac.uk)] and Michael Pittman [[mdpittman@hotmail.com](mailto:mdpittman@hotmail.com)], Department of Earth Sciences, University College London, Gower Street, London, WC1E 6BT, UK; Jonah Choiniere [[jonah.choiniere@gmail.com](mailto:jonah.choiniere@gmail.com)], Department of Biological Sciences, George Washington University, 2023 G Street NW, Washington, DC 20052, USA; Qingwei Tan [[fristtan@sina.com](mailto:fristtan@sina.com)] and Lin Tan, Long Hao Institute of

Geology and Paleontology, Hohhot, Nei Mongol 010010, China; Dong Xiao, Department of Land and Resources, Linhe, Nei Mongol 015000, China.

 [Accepted manuscript \(2,319.9 kB\)](#)

This is a PDF file of the manuscript  
that has been accepted for publication.  
This file will be reviewed by the authors and editors  
before the paper is published in its final form.  
Please note that during the production process errors  
may be discovered which could affect the content.  
All legal disclaimers that apply to the journal pertain.

# Osteology of the alvarezsauroid *Linhenykus monodactylus* from the Upper Cretaceous Wulansuhai Formation of Inner Mongolia, China, and comments on alvarezsauroid biogeography

XING XU, PAUL UPCHURCH, QINGYU MA, MICHAEL PITTMAN, JONAH CHOINIERE, CORWIN SULLIVAN, DAVID W. E. HONE, QINGWEI TAN, LIN TAN, DONG XIAO, and FENGLU HAN

Xu, X., Upchurch, P., Ma, Q., Pittman, M., Choiniere, J., Sullivan, C., Hone, D.W.E., Tan, Q., Tan, L., Xiao, D., and Han, F. 201X. Osteology of the alvarezsauroid *Linhenykus monodactylus* from the Upper Cretaceous Wulansuhai Formation of Inner Mongolia, China, and comments on alvarezsauroid biogeography. *Acta Palaeontologica Polonica* 5X (X): xxx-xxx.  
<http://dx.doi.org/10.4202/app.2011.0083>

The alvarezsauroid *Linhenykus monodactylus* from the Upper Cretaceous of Inner Mongolia, China is the first known monodactyl non-avian dinosaur, providing important information on the complex patterns of manual evolution seen in alvarezsauroids. Here we provide a detailed description of the osteology of this taxon. *Linhenykus* shows a number of features that are transitional between parvicursorine and non-parvicursorine alvarezsauroids, but detailed comparisons also reveal that some characters had a more complex distribution. We also use event-based tree-fitting to perform a quantitative analysis of alvarezsauroid biogeography incorporating several recently discovered taxa. The results suggest that there is no statistical support for previous biogeographic hypotheses that favour pure vicariance or pure dispersal scenarios as explanations for the distributions of alvarezsauroids across South America, North America and Asia. Instead, statistically significant biogeographic reconstructions suggest a dominant role for sympatric (or ‘within area’) events, combined with a mix of vicariance, dispersal and regional extinction. At present the alvarezsauroid data set is too small to completely resolve the biogeographic history of this group: future studies will need to create larger data sets that encompass additional clades.

**Key words:** Late Cretaceous, Wulansuhai Formation, Parvicursorinae, Theropoda, alvarezsauroid biogeography, Treefitter, dispersal, vicariance, sympatry

Xing Xu [xingxu@vip.sina.com], Qingyu Ma [maqingyu.ivpp@gmail.com], Corwin Sullivan [csullivan@ivpp.ac.cn], David W.E.Hone [dwe\_hone@yahoo.com], and Fenglu Han [hfl0501@gmail.com], Key Laboratory of Evolutionary Systematics of Vertebrates, Institute of Vertebrate Paleontology & Paleoanthropology, Chinese Academy of Sciences, 142 Xiwai Street, Beijing 100044, China;

Paul Upchurch [p.upchurch@ucl.ac.uk] and Michael Pittman [mdpittman@hotmail.com], Department of Earth Sciences, University College London, Gower Street, London, WC1E 6BT, UK; Jonah Choiniere [jonah.choiniere@gmail.com], Department of Biological Sciences, George Washington University, 2023 G Street NW, Washington, DC 20052, USA;

Qingwei Tan [firsttan@sina.com] and Lin Tan [6535075], Long Hao Institute of Geology and Paleontology, Hohhot, Nei Mongol 010010, China;

Dong Xiao, Department of Land and Resources, Linhe, Nei Mongol 015000, China.

Received 19 July 2011, accepted 1 December 2011, available online 13 December 2011.

## Introduction

With only one exception (Choiniere et al. 2010), all known alvarezsauroid theropods are restricted to Upper Cretaceous deposits (Bonaparte 1991; Novas 1997; Naish and Dyke 2004; Kessler et al. 2005; Martinelli and Vera 2007; Longrich and Currie 2009; Salgado et al. 2009). Among these Late Cretaceous alvarezsauroids, Asian species possess the most specialized body-plans, and are best known from the Upper Cretaceous of Mongolia. The Mongolian alvarezsauroid assemblage includes taxa, such as *Mononykus olecranus* from the Nemegt Formation (Perle et al. 1993; Perle et al. 1994) and *Shuvuuia deserti* from the Djadokhta Formation (Chiappe et al. 1998), whose systematic positions have been highly debated. Djadokhta-equivalent deposits in the neighboring Chinese region of Inner Mongolia (Jerzykiewicz et al. 1993) contain a broadly similar vertebrate fauna, but few alvarezsauroid specimens have been recovered from Inner Mongolia.

In the 2008 summer field season, a joint expedition team from the Institute of Vertebrate Paleontology & Paleoanthropology, the Longhao Institute of Geology and Paleontology, and the Bureau of Land and Resources of Bayannur, Inner Mongolia prospected in the Upper Cretaceous dinosaur-bearing deposits of the Bayan Mandahu area in north-central Inner Mongolia. On August 14<sup>th</sup>, two of the authors (MP and JC) discovered and collected some small theropod bones in the red beds at the Gate Locality (Jerzykiewicz et al. 1993), and they revisited the site and collected a few more elements belonging to the same specimen on August 18<sup>th</sup>. The specimen was found on a low outwash plain east of the high cliffs at the Gate Locality, and was fully exposed on a surface of extensively weathered red massive sandstone directly below a thick, resistant sandstone layer (less than 1 m in thickness) with numerous calcite-rich concretions. Digging below the exposed bone failed to reveal additional elements.

The preservation and distribution of the bones suggest that the specimen was originally preserved in a concretion that had fully weathered out on the surface of the outwash plain. The major elements of the skeleton were clustered within a 30 cm radius, while some smaller pieces discovered during the initial search on the 14th had washed down slope to a distance of less than 1 m. During the second site visit a wider survey revealed a few further elements up to 4m from the skeleton. A disarticulated and highly fragmentary turtle specimen was found ~1m from the specimen, but the extensive weathering of the turtle elements suggests that they had been exposed for a much greater time and were not associated with the theropod. The presence of a robust medial manual digit and a fused, block-like carpometacarpus identify this specimen as an alvarezsaurid

theropod, but several features distinguish it from other known alvarezsaurids and a phylogenetic analysis places it at the base of the derived clade Parvicursorinae (Xu et al. 2011d). Furthermore, only one metacarpal of this specimen possesses manual phalanges, indicating that this animal has only one phalanx-bearing digit and thus represents the first known monodactyl non-avian dinosaur. This specimen was the subject of a brief description (Xu et al. 2011d), however, given the significance of this taxon for understanding alvarezsauroid evolution, we provide here a more detailed account of the osteological features of the specimen. Furthermore, we provide in the present paper a quantitative analysis of alvarezsauroid biogeography incorporating information from this find.

## **Systematic Palaeontology**

### **Dinosauria Owen, 1842**

#### **Theropoda Marsh, 1881**

#### **Alvarezsauridae Bonaparte, 1991**

#### **Parvicursorinae Karhu & Rautian 1996**

The Parvicursorinae was originally proposed by Karhu and Rautian (1996), but a phylogenetic taxonomic definition for the clade was first proposed by Choiniere et al (2010), which is a node-based definition (Choiniere et al. 2010). *Linhenykus* and other recently reported parvicursorines such as *Albertonykus* (Longrich and Currie 2009) and *Xixianykus* (Xu et al. 2010) are morphologically very similar to members of this node-based Parvicursorinae, but they are excluded from the node-based clade based on the recovered alvarezsauroid phylogeny. We believe that it is not necessary to establish a new clade and the most informative option is to treat Parvicursorinae as a stem-based taxon, allowing for the inclusion of *Linhenykus* and other taxa (Xu et al. 2011a, 2011b). Thus, we define Parvicursorinae as the most inclusive clade including *Parvicursor remotus* but not *Patagonykus puertai*

*Revised Parvicursorinae diagnosis*--Dorsal vertebrae opisthocoelous and without hyposphene-hypantrum articulations, dorsal parapophyses elevated to level of diapophyses, dorsal infradiapophyseal fossae hypertrophied, posterior sacral vertebrae with hypertrophied ventral keels, anterior caudal vertebrae with anteriorly displaced transverse processes, metacarpal II that is mediolaterally wider than proximodistally long and dorsoventrally shallow, bears two articular

facets on the proximal surface, and lacks collateral ligamental fossae, manual ungual II with ventral axial groove and without flexor tubercle, tibial distal end with lateral malleolus anteroposteriorly expanded, astragalar ascending process L-shaped, and specialized arctometatarsalian condition with metatarsal III shorter than metatarsals II and IV. Other possible parvicursorine synapomorphies include: posterior dorsal vertebrae with small and posterodorsally oriented neural spines; biconvex vertebra near posterior end of dorsal series; keeled and boatlike sternum with median groove along midline; manual phalanx II-2 longer than II-1; supracetabular crest of ilium more prominent anteriorly than posteriorly; metatarsus longer than femur; metatarsals II and IV subequal in length; and pedal digit III more slender than digits II and IV.

***Linhenykus monodactylus* Xu, Sullivan, Pittman, Choiniere, Hone, Upchurch, Tan, Xiao, Tan, And Han, 2011**

*Diagnosis.*--A small parvicursorine apomorphically possessing a transversely compressed metacarpal III without a distal articular surface; also differs from all other parvicursorines in having a longitudinal ventral furrow along the entire length of each cervical centrum, diapophyseal ridges on each cervical vertebra that extend to the posterodorsal rim of the centrum, extremely weak, ridge-like epipophyses on the postzygapophyses of the middle cervical vertebrae, large pneumatic foramina in the mid-dorsal vertebrae, and anteriormost caudal vertebrae whose centra are amphiplatyan and whose neural spines are located completely posterior to the neural pedicles.

*Material.*--The taxon is only represented by the holotype specimen, IVPP (Institute of Vertebrate Paleontology & Paleoanthropology) V17608, a partial postcranial skeleton including 4 partial cervical vertebrae, 3 partial dorsal vertebrae, 5 partial sacral vertebrae, 13 caudal vertebrae, a fragmentary anterior or middle chevron, part of the left scapulocoracoid, a nearly complete sternum, the distal ends of the right humerus and left ulna, the left radiale, the left metacarpals II and III and the phalanges of the left digit II, part of the right metacarpal II, the incomplete right phalanx II-1 and complete right phalanx II-2, part of the left ilium, the proximal end of the left pubis, the almost complete right and left femora and tibiae, parts of the right and left astragalus-calcaneum complexes, the nearly complete left metatarsus, the distal end of the right metatarsal IV, and all of the left pedal phalanges other than IV-4 and IV-5, although phalanges II-2, III-1 and III-3 are only partially preserved (Fig. 1).

## Figure. 1

*Locality and Horizon.*--Coordinates in decimal degrees: N41.74392 E106.74436. Bayan Mandahu, "Gate Locality", Wulansuhai Formation, Campanian, Late Cretaceous (Jerzykiewicz et al. 1993).

## Description and comparisons

The specimen is small, with an estimated femoral length only slightly exceeding 70 mm. On the basis of this estimate, IVPP V17608 is only about half of the size of the holotype of *Mononykus olecranus* (Perle et al. 1993; Perle et al. 1994), but is considerably larger than that of *Parvicursor remotus* (Suzuki et al. 2002). IVPP V17608 is estimated to have a body mass of approximately 450 g based on an empirical equation using femoral length as a predictor (Christiansen and Fariña 2004). All of the preserved vertebrae have completely closed neurocentral sutures. However, intercentral sutures are evident between successive sacral vertebrae, metacarpal III is not fused to metacarpal II, and the proximal tarsals are not completely co-ossified with the tibia. Although caution is warranted when relying on neurocentral fusion as a sole indicator of ontogenetic stage (Irmis 2007), the presence of other ontogenetically-informative fusion in the vertebral and appendicular skeleton (above) suggests a relatively late ontogenetic stage for IVPP V17608, with sub-adult being more likely than adult.

## Axial Skeleton

The axial skeleton is represented by 4 partial cervical vertebrae, 3 partial dorsal vertebrae, 4 partial sacral vertebrae, and 13 caudal vertebrae. Most of the preserved neural arches are incomplete, and some vertebrae are only represented by broken centra.

*Cervical vertebrae.*--Four cervical vertebrae are preserved, but only one is relatively complete. They might represent anterior and middle cervical vertebrae, based on the morphology of the ventral surfaces of the centra and the locations of the postzygapophyses (Fig. 2).

## Figure. 2

The preserved cervical centra are strongly opisthocoelous, a condition also seen in *Shuvuuia* and *Mononykus* (Chiappe et al. 2002a) but not in *Haplocheirus* (Choiniere et al. 2010) and *Alvarezsaurus* (Bonaparte 1991). Unknown cervical articular geometries for other alvarezsauroids makes it difficult to reconstruct the distribution of cervical opisthocoely across the alvarezsauroid tree but it appears to have been present by at least the Parvicursorinae node although cervical opisthocoely has also been proposed, tentatively, to be present in *Patagonykus* (Novas 1996, Novas



1997, Chiappe et al. 2002a). Future discoveries will be important in testing this hypothesis. The cervicals also resemble their counterparts in other alvarezsaurids in that the condyle on the anterior surface of each cervical centrum is distinctly smaller than the articular surface. The cervical centra are mediolaterally compressed in such a way that their lateral surfaces are moderately concave, and their ventral surfaces are narrow as in *Mononykus*, *Parvicursor*, and probably *Patagonykus* (Novas 1997). In lateral view, the cervical centra are long and low, as in other alvarezsauroids. An oblique ridge (posterior centrodiapophyseal lamina) runs from the diapophysis to the posterodorsal corner of each middle cervical centrum. In ventral view, two sharp ridges run along the edges of the centrum, flanking a midline furrow on the narrow ventral surface. These two ridges approach each other near the mid-length of the centrum, so that the furrow widens anteriorly and posteriorly. In *Shuvuuia* and *Mononykus*, a similar furrow is present, but occupies only the anterior half of the ventral surface (Chiappe et al. 2002a). In *Linhenykus* carotid processes appear to be present, but are confluent with the anterior ends of the ridges. Carotid processes are known in derived alvarezsauroids *Shuvuuia* and *Mononykus*, and some ornithomimosaurids, oviraptorosaurs, dromaeosaurids, troodontids and avialans as well. Subcircular pneumatic foramina are located immediately posterior to the parapophyses as in *Alvarezsaurus* and *Shuvuuia*. Pneumatic foramina have not been reported in *Mononykus* or *Parvicursor*. The foramina are proportionally large (about 3 mm in diameter on a cervical centrum with an estimated length of 9 mm), but this appears to be partly an artifact of preservation.

The neural pedicles are mediolaterally broad and dorsoventrally low. The anterior edge of each pedicle is flush with the anterior articular surface (excluding the condyle) of the centrum, but the posterior edge is located considerably anterior to the posterior articular surface. The parapophyses are low, laterally projecting eminences, and the diapophyses are represented by thin tubercles that are connected to the prezygapophyses by prezygodiapophyseal laminae. The prezygapophyses are set well lateral to the centra. Their articular surfaces face nearly medially and only slightly dorsally, suggesting that lateral bending within the cervical column was rather restricted. The prezygapophyseal processes have a strong dorsal orientation, particularly in the more posterior cervical vertebrae in which the prezygapophyseal processes barely protrude anteriorly beyond the intercentral articulation. The postzygapophyseal processes diverge strongly away from the midline and also have a strong dorsal orientation. In the anterior cervical vertebrae the postzygapophyseal processes are located anterior to the intercentral articulation, whereas in the

middle ones the postzygapophyseal process are at the level of the intercentral articulation. The postzygapophyses each have a nearly straight medial edge and a convex lateral edge in dorsal view, as in other Asian alvarezsaurids (Chiappe et al. 2002a). In *Alvarezsaurus* the postzygapophyses are paddle-shaped due to the presence of a convex medial edge (Bonaparte 1991). No epipophyses are apparent on the postzygapophyses of the posterior cervical vertebrae of *Linhenykus*, but extremely weak, ridge-like epipophyses are present in the middle cervical vertebrae. The neural spines of the middle cervical vertebrae are extremely low and very short anteroposteriorly, and possess shallow interspinous ligament fossae on their posterior margins. The neural canal is proportionally large in the cervical centra, a feature of alvarezsaurids generally (Chiappe et al. 2002a).

Cervical ribs are not preserved, but there is no evidence that they were fused to the cervical vertebrae. In *Shuvuuia* (IGM 100/977), the ribs of the anterior cervical vertebrae are partially fused to the diapophyses and fully fused to the parapophyses.

*Dorsal vertebrae.*--One of the three preserved dorsal vertebrae probably comes from the middle part of the dorsal region, while the other two are preserved in articulation with each other and probably represent posteriormost dorsal vertebrae (Fig. 3). The neurocentral sutures are all closed, leaving no visible traces. Each dorsal vertebra has a mediolaterally compressed centrum with a sharp ventral midline ridge, as in *Mononykus* (Perle et al. 1994) but in contrast to *Shuvuuia* (Chiappe et al. 2002a; Suzuki et al. 2002) and *Xixianykus* (Xu et al. 2010) in which the posteriormost dorsal centra are transversely narrow but not ventrally ridged. The articular surfaces of the dorsal centra are sub-triangular in outline, unlike the ovoid ones in *Shuvuuia* (IGM 100/977) and *Xixianykus* (Xu et al. 2010). The middle dorsal vertebra is opisthocoelous, with a convex, knob-like anterior projection that is significantly smaller than the articular surface. The condyle appears to be even smaller, relative to the anterior intercentral articular surface, in the presacral vertebrae of other known parvicursorines such as *Mononykus* and *Shuvuuia* (Perle et al. 1994, Chiappe et al. 2002a). The centrum of the middle dorsal vertebra is slightly greater in transverse width than in dorsoventral depth, unlike *Shuvuuia* (IGM 100/977), which has transversely much wider posterior articular surface relative to the dorsoventral depth. Large openings, which are probably pneumatic foramina, are present on both sides of the centrum, which terminate on the neurocentral suture and have a diameter equal to approximately half the length of the centrum. The left and right foramina are continuous across the midline of the centrum, but this condition is presumably a result of postmortem damage. This is the first known example of a pneumatic dorsal vertebra among

alvarezsauroids (Chiappe et al. 2002a, Choiniere et al. 2010). The posterior dorsal vertebrae probably represent the last and the second to last in the dorsal sequence. The penultimate dorsal has a biconvex centrum. Biconvex dorsal vertebrae are also known in *Xixianykus* (Xu et al. 2010), *Mononykus* and *Shuvuuia* (Chiappe et al. 2002a), but in *Xixianykus* (Xu et al. 2010), and probably *Mononykus* and *Shuvuuia* (Chiappe et al. 2002a) it is the last dorsal vertebra that has a biconvex centrum. The last dorsal has an anteriorly concave centrum, but its posterior end is broken. Neither posterior dorsal vertebra bears a pneumatic fossa or foramen on the lateral surface of the centrum. The anterior and posterior articular surfaces of the penultimate dorsal vertebra each bear a condyle that occupies the whole area of the articular surface, in contrast to the reduced anterior condyle of the middle dorsal vertebra, a condition that is present in all the dorsals of *Mononykus* and *Xixianykus* (Perle et al. 1994; Xu et al. 2010). The centrum of the last dorsal vertebra is considerably larger than the other preserved dorsal centra, and is mediolaterally wider than dorsoventrally deep.

### Figure. 3

The parapophyses are located on small projections at the bases of the prezygapophyseal processes, and lie approximately on a level with the diapophyses as in other parvicursorines (Chiappe et al. 2002a; Longrich and Currie 2009). A horizontal paradiapophyseal lamina (Wilson 1999) overhangs the large pneumatic foramen on the preserved middle dorsal vertebra, but is lacking in the penultimate dorsal vertebra. The neural arches of all three dorsal vertebrae are low in lateral view. The prezygapophyses of the middle dorsal vertebra are considerably lower than the postzygapophyses, which are very close to the midline. The neural spine is small and low and posterodorsally oriented on the middle dorsal vertebra and probably also on the posterior dorsal vertebrae, though the neural spines of the posterior dorsals are not complete. In *Mononykus* and *Shuvuuia* (Perle et al. 1994; Chiappe et al. 2002a), the neural spines of the middle dorsals are large and high. As in other parvicursorines (Chiappe et al. 2002a; Longrich and Currie 2009), there are no hyposphene-hypantrum articulations unlike the basal alvarezsauroids *Haplocheirus* and *Patagonykus* where such articulations are present (Novas 1997; Choiniere 2010). The neural canal is large relative to the centrum as in other alvarezsaurids (Chiappe et al. 2002a).

*Sacral vertebrae.*--One isolated sacral vertebra and two sets of two fragmentary sacral vertebrae in articulation are present (Fig. 4). Two of the fragmented ends fit closely together, suggesting that the two sets might actually represent three consecutive sacral vertebrae, but this cannot be confirmed.

Therefore, a minimum of four and a maximum of five sacral centra are represented. The isolated one is likely to be the second to last sacral vertebra and the other three are likely to be the third, fourth and fifth to last one. For convenience, we refer to these sacral vertebrae as sacral A through sacral D, with A being the most anterior in the sequence. *Shuvuuia* and *Xixianykus* have seven sacral vertebrae (Chiappe et al. 2002a; Xu et al. 2010), but more primitive alvarezsaurids have as few as five sacrals (Novas 1996; Chiappe et al. 2002a), so we cannot be sure how many were present in *Linhenykus*. All of the preserved sacral vertebrae are opisthocoelous, though sacral D is only very weakly so. The opisthocoelous condition appears to be present in at least the first sacral vertebra of *Parvicursor* (Karhu and Rautian 1996; Chiappe et al. 2002a). Most other alvarezsaurids, including *Patagonykus* and *Xixianykus*, have procoelous sacral vertebrae (Novas 1996; Chiappe et al. 2002a; Xu et al. 2010). All of the preserved sacral centra are laterally compressed as in other alvarezsaurids (Chiappe et al. 2002a), and the compression becomes stronger posteriorly. However, the anterior ends of sacrals B and C are only slightly compressed, so that they form a prominent anterior margin relative to the laterally compressed central main body. This feature is present to a degree in the first sacral vertebrae of other alvarezsaurids such as *Xixianykus* (Xu et al. 2010), but otherwise is not characteristic of the group. The mediolateral width/dorsoventral height ratio of the anterior end of sacral B is about 1.9. Relatively wide anterior and middle sacral centra are also known in *Xixianykus* (Xu et al. 2010). The anterior articular surfaces of the four sacral vertebrae are semi-circular in outline, with the mediolateral width much greater than the dorsoventral height. The posterior articular surfaces of sacrals A and B are sub-trapezoidal in outline, with the mediolateral width again much greater than the dorsoventral height. However, the posterior surface of sacral D is triangular in outline, with the mediolateral width much smaller than the dorsoventral height. There appears to be a groove on the ventral surface of sacral A, which extends posteriorly onto the ventral surface of sacral B. A ventral groove is also known in *Alvarezsaurus* (Bonaparte 1991), *Xixianykus* (Xu et al. 2010), and an unnamed alvarezsaurid from Mongolia (Longrich and Currie 2009), though the length of the groove varies among these taxa. The preserved anterior half of sacral C is ventrally keeled, whereas the ventral surface of sacral D is strongly keeled over all but the anteriormost part of its length. The sacral rib of sacral B arises from nearly the whole length of the lateral surface of the centrum, but is slightly offset towards the anterior end of the vertebra. The sacral fenestrae appear to be large, and the successive sacral ribs appear not to be fused to form a large lamina as in *Xixianykus* (Xu et al. 2010). In contrast to the

smooth transition from the lateral surface of the centrum to the ventral surface of the sacral rib, a distinct notch is visible in anterior view between the lateral edge of the anterior end of the centrum and the ventral surface of the sacral rib.

#### **Figure. 4**

*Caudal vertebrae.*--There are 13 caudal vertebrae preserved, some of which are fragmentary (Figs. 5 and 6). We have numbered these caudal vertebrae in an anatomically anteroposterior order (C1 through C13), although they may not represent a continuous series. Position in the numbering sequence was determined on the basis of size, in addition to the relative development and positioning of such features as neural spines, transverse processes, and ventral keels. C1-3 probably represent the true first through third caudal vertebrae; C4-6 possibly come from the middle region of the anterior caudal series; C7-9 from the posterior region of the anterior caudal series; C10-12 from the middle caudal series; and C13 from the anterior region of the posterior caudal series.

#### **Figure. 5**

All of the preserved caudal vertebrae are mediolaterally compressed, and the compression is greater in the more anterior caudal vertebrae. C1 displays an extremely weak opisthocoelous condition; C2 has a slightly convex anterior intercentral articular surface and a prominent condyle on the posterior intercentral articular surface; and all of the other caudal vertebrae are procoelous. In other alvarezsaurids including *Alvarezsaurus* and *Patagonykus*, all of the caudal vertebrae are procoelous (Novas 1996; Chiappe et al. 2002a). Most of the preserved caudal vertebrae, with the exception of C1-3, are marked by a longitudinal furrow that runs along the entire ventral surface of the centrum and is bordered laterally by two ventral keels. This feature is also known in some other alvarezsaurids such as *Shuvuuia* (Chiappe et al. 2002a). All of the preserved neural arch pedicles are positioned anteriorly on the centra as in other alvarezsaurids (Chiappe et al. 2002a). The pedicles of the anterior caudals (C1-9) are each restricted to the anterior half of the corresponding centrum, but the pedicles of the more posterior caudal vertebrae each cover most of the corresponding centrum's length. The intercentral foramina are large due to the strong dorsal orientation of the zygapophyses.

#### **Figure. 6**

C1 preserves only the centrum. It is sub-equal in anteroposterior length to the second last sacral vertebra, but is much greater in central height. The centrum is strongly compressed laterally, and the ventral margin forms a sharp keel that renders the anterior and posterior intercentral

articular surfaces triangular in outline. C2 and C3 slightly exceed C1 in anteroposterior length. C2 and C3 each have a sharp ventral keel like C1, but only the anterior intercentral articular surface of C2 shares the triangular outline of the intercentral articular surfaces of C1. Caudal vertebrae with sharp ventral keels are also present in *Shuvuuia*, *Parvicursor*, *Xixianykus*, and *Alvarezsaurus*, but there are only two such caudals known in *Shuvuuia* and only one each in *Parvicursor*, *Xixianykus*, and *Alvarezsaurus* (Chiappe et al. 2002a, Xu et al. 2010). The posterodorsally-oriented neural spine of C2 is short anteroposteriorly and low dorsoventrally. The neural spine is located completely posterior to the neural pedicles, lying at the level of the postzygapophyses. The same condition is seen in some other parvicursorines such as *Shuvuuia* (Chiappe et al. 2002a), though in other taxa the neural spine is slightly more anteriorly located. C3 exhibits transverse processes located at the bases of the prezygapophyseal processes. The long axis of the cross section of each transverse process is slightly oblique (anterodorsally-posteroventrally). As in *Xixianykus* (Xu et al. 2010) and *Shuvuuia* (Chiappe et al. 2002a), the bases of the transverse processes are anteriorly located, even projecting slightly beyond the anterior articular surface of the centrum. The prezygapophyseal processes have a strong dorsal orientation, and extend considerably beyond the intercentral articulation.

C4-C13 are similar to each other in general morphology, though there are minor structural variations among the individual vertebrae. As in parvicursorines but unlike in *Alvarezsaurus* and *Haplocheirus* (Bonaparte 1991; Choiniere 2010; Choiniere et al. 2010), the vertebrae gradually become shorter anteroposteriorly and lower dorsoventrally along the caudal series, although C10 is longer than the preceding vertebra. The anterior intercentral articular surfaces of C3-13 are sub-trapezoidal in outline. The neural arch pedicles extend further posteriorly on the centra of the posterior caudal vertebrae than on the centra of the anterior ones. Transverse processes are present in all preserved caudal vertebrae, though they become greatly reduced in size posteriorly. The position of the transverse processes becomes more posterior, and slightly more ventral, in the more posterior caudal vertebrae. The transverse processes are located close to the anterior intercentral articular surface in C4, but are close to the posterior articular surface in C13. These processes are posterolaterally oriented throughout the caudal series, as in *Shuvuuia* and *Alvarezsaurus* (Chiappe et al. 2002a). In *Parvicursor*, the transverse processes have been interpreted as anterolaterally oriented (Karhu and Rautian 1996). The long axis of the cross section of each transverse process remains clearly oblique (oriented anterodorsally-posteroventrally) as far back as C9, but becomes nearly horizontal in C10-13. The prezygapophyseal processes retain a strong dorsal orientation throughout

the series, and the articular facets of both the pre- and postzygapophyses are steeply inclined throughout the caudal sequence. The prezygapophyseal processes become shorter in the posterior caudals, but extend beyond the intercentral articulation even in C12, the last caudal vertebra in which prezygapophyses are preserved. The postzygapophyses assume a more posterior location in the posterior caudal vertebrae, projecting just beyond the intercentral articular surface in C13. The neural spines of C4-C13 are posteriorly positioned, occurring at the level of the postzygapophyses as in C2 and C3. Passing posteriorly along the series, the neural spines become lower dorsoventrally but longer anteroposteriorly. In C13 the neural spine is still visible in the form of a sharp, low ridge, and extends over about two-thirds of the total length of the centrum. The posterior margin of the neural spine of C13 is much thicker transversely than the anterior margin.

A fragmentary chevron is preserved between C7 and C8. A proximal bridge connects the left and right halves of the chevron dorsal to the hemal canal, and the anterior margin of the proximal end is slightly bifurcated. The distal portion of the chevron is broken away.

### **Pectoral girdle and sternum**

*Scapula and coracoid.*--Unlike those of other alvarezsauroids, the scapula and coracoid of V17608 are fused together, although the evidence for this comes exclusively from a small preserved portion of the left scapulocoracoid (Figs. 7A). The preserved scapulocoracoid is reminiscent of the scapula and coracoid of basal alvarezsauroids (Choiniere 2010; Choiniere et al. 2010), rather than those of other parvicursorines (Chiappe et al. 2002a), in having a weakly developed glenoid lip that protrudes only slightly beyond the ventral edge of the scapular blade. In most other parvicursorines (Chiappe et al. 2002a), the glenoid lip is much more prominent. The small preserved portion of the acromion process suggests an abrupt dorsal expansion of the scapular blade. The glenoid fossa faces posteroventrally as in other alvarezsauroids (Chiappe et al. 2002a; Choiniere et al. 2010). The part of the scapular blade adjacent to the glenoid is convex laterally and flat medially, with a thick, somewhat rounded ventral margin and a transversely narrow dorsal margin that bears a sharp longitudinal ridge. The broken surface of the scapular blade reveals a hollow interior, though this is possibly due to erosion. The coracoid is represented only by a small piece of bone fused to the scapula in the glenoid region, and little can be said about its morphology.

### **Figure. 7**

*Sternum.*--The sternum is a single, fused element lacking any trace of a midline suture (Figs. 7B1 and B2). It appears to be almost complete, though its left margin is slightly broken. In general form it is a small, stout, bone, tapering to a broad posterior point. The sternum is only slightly anteroposteriorly longer than it is transversely wide, whereas in other Asian parvicursorines this element is considerably longer than wide (Perle et al. 1994; Chiappe et al. 2002a). The dorsal surface of the sternum is transversely concave, a feature also seen in other Asian alvarezsaurids (Perle et al. 1994; Chiappe et al. 2002a). The ventral surface of the sternum is pitted, and bears a moderately developed carina (sternal keel) that bifurcates anteriorly into two lateral crests enclosing a median groove. This region is slightly eroded in IVPP V17608, so that the degree of development of the crests and groove cannot be fully determined. The carina is much weaker than in other parvicursorines (Perle et al. 1994; Chiappe et al. 2002a), representing little more than a sharp line of inflection between the right and left halves of the sternum. The maximum depth along the midline of the sternum is less than 30% of the maximum width of the sternum, whereas the two measurements are subequal in other parvicursorines. The medial groove is, however, proportionally longer than in other parvicursorines (Perle et al. 1994; Chiappe et al. 2002a). The anterior margin of the sternum is convex, without a midline indentation as seen in *Mononykus* (Perle et al. 1994). As in *Shuvuuia* and *Mononykus* (Perle et al. 1994; Chiappe et al. 2002a), the sternum lacks facets for rib articulation. If ossified sternal ribs were present, they evidently left no impressions on the bony sternum.

### **Forelimb**

*Humerus.*--Only the distal end of a right humerus is preserved (Figs. 8A1-A3). However, it is clear that the distal end curves anteriorly relative to the shaft in lateral view, a feature also seen in *Mononykus* and a variety of other theropods including more primitive tetanurans such as *Baryonyx*. The shaft is truncated at a point 7 mm from the distal end, revealing a sub-oval cross section. A large condyle occupies the whole medial side of the distal end, so that there is no distinct entepicondyle of the kind present in *Patagonykus* (Novas 1997). The distal condyle projects mainly anteriorly and is subtriangular in anterior view as in *Mononykus* (Perle et al. 1994), although in *Mononykus* the condyle extends further proximally than in *Linhenykus*. The articular surface of the distal condyle appears to continue a long way onto the distal surface of the humerus. Proximal to the distal condyle, the shaft of the humerus is relatively flat. The condyle is also anteriorly



prominent close to the medial side of the humerus, and is sub-triangular in outline in distal view. On the distal surface of the humerus, the condyle's lateral border is defined by an oblique crest that projects further distally than the main part of the condyle. In distal view, a small posterior notch separates the crest from the anteroposteriorly expanded main body of the condyle, as in *Mononykus* (Perle et al. 1994). The posterior surface of the distal end is only slightly concave, a condition intermediate between those seen in other Asian alvarezsaurids and in *Patagonykus* (Chiappe et al. 2002a).

### **Figure. 8**

*Ulna.*--A long bone fragment is tentatively identified as the distal end of the left ulna (Figs.8B1-B3). The shaft, broken through approximately 10 mm from the distal end, is sub-circular in cross section. In anterior or posterior view, the shaft curves medially. The shaft expands anteroposteriorly toward the distal end, close to which is a shallow fossa on the medial surface. As in other alvarezsaurids (Chiappe et al. 2002a), the distal end bears a large carpal trochlea, on the posteromedial corner of which is a distinct, triangular articular facet that extends further proximally on the medial surface than does the main part of the trochlea. In contrast to other alvarezsaurids (Chiappe et al. 2002a), there appears to be an indentation in the middle of the distal trochlear surface, between more prominent anterior and posterior areas.

*Manus.*--The preserved manual elements (Fig. 9) include the left radiale, left metacarpals II and III, left digit II, incomplete right metacarpal II, incomplete right phalanx II-1 and complete right phalanx II-2. Note here we refer to the digits of the tetanuran hand as II-IV (Kundrát et al. 2002, Xu et al. 2009), rather than as I-III as preferred by many previous workers (Gauthier 1986, Chatterjee 1998; Wagner and Gauthier 1999; Vargas and Fallon 2005; Vargas et al. 2008; Tamura et al. 2011). All of the elements belonging to the left manus and carpus appear to have weathered out of a single nodule, in which they were preserved close to a state of natural articulation.

### **Figure. 9**

The left radiale is a small, ovoid bone, with a maximum diameter of about 2 mm. No unfused proximal carpal elements have previously been reported in any alvarezsaurid (Chiappe et al. 2002a). What appears to be the proximoventral surface of the radiale bears a distinct fossa. A separate 'semilunate' carpal is absent, but is probably fused to metacarpal II as suggested by previous studies (Chiappe et al. 2002a; Choiniere 2010; Choiniere et al. 2010). This inference is supported by the close topological resemblance between the middle part of the proximal articular

surface of the main carpometacarpal element (formed by metacarpal II and the ‘semilunate’ carpal in *Linhenykus*), which is transversely trochleated and strongly convex in dorsal or ventral view, and the corresponding surface of the ‘semilunate’ carpal in many less specialized tetanurans (Chure 2001). However, there is no visible suture between the semilunate carpal and metacarpal II, suggesting that fusion occurred very early in ontogeny.

The main carpometacarpal element is proximodistally short, mediolaterally broad, dorsoventrally shallow, and subpentagonal in dorsal or ventral outline. It is proportionally much narrower transversely than its counterpart in *Mononykus* (length/width ratio about 0.80 in *Linhenykus*, compared to about 0.60 in *Mononykus*). Three articular facets are present on the proximal surface of the main carpometacarpal element. The middle and lateral facets appear to correspond to the “medial facet” and “central facet” of Chiappe et al. (2002), a terminology we adopt here (the lateral facet defined by Chiappe et al. is formed exclusively by metacarpal IV, which is probably absent in *Linhenykus*). However, a distinctive accessory facet is present medial to the medial facet in IVPP V17608, and an equivalent surface is also present in *Mononykus* but was not separately considered by Chiappe et al. (2002). We refer to this facet as the “accessory medial facet”. The accessory medial facet comprises a relatively deep fossa and faces more medially than proximally. It is separated from the medial facet by a dorsoventral constriction of the proximal surface of the main carpometacarpal element. The medial facet is a transversely grooved, elongate trochlea in proximal view, and represents the area that corresponds to the proximal surface of the ancestral semilunate carpal. This trochlear structure is obliquely oriented, tilting in a ventromedial-dorsolateral direction so that the groove extends slightly onto the dorsal surface of the main carpometacarpal element. In dorsal view, the medial facet is proximally convex. As in *Mononykus*, the proximal articular surface is dorsoventrally constricted between the medial and central facets (Perle et al. 1994). The central facet is a large, distinct fossa. Interestingly, despite the almost identical morphology of the proximal articular surface of the main carpometacarpal in *Linhenykus* and *Mononykus*, this concave central facet has a straight dorsal border and a convex ventral border in *Linhenykus*, while the opposite is true in *Mononykus* (Perle et al. 1994).

The distal end of metacarpal II bears two prominent condyles separated by a broad, well-developed groove. Collateral ligamental fossae are absent, as in other alvarezsaurids including *Patagonykus* (Novas 1997). The medial condyle of the distal end is more dorsally prominent than the lateral condyle. However, the lateral condyle extends significantly more distally than the lateral

one as in *Haplocheirus*, *Patagonykus*, and many other non-avian theropods (Choiniere 2010, Choiniere et al. 2010), whereas in *Mononykus* the distal condyles are approximately equal in size (Chiappe et al. 2002a). The medial condyle is obliquely oriented and its dorsal surface is transversely narrow. The lateral condyle has limited dorsal exposure and is transversely broad. This condyle is located at the lateral edge of the bone, so that there is no accessory process situated proximolateral to it as in *Mononykus* (Perle et al. 1994). The entire lateral surface of metacarpal II forms a sharply defined, flat articular facet for metacarpal III, as in *Mononykus* and *Shuvuuia* (Perle et al. 1994; Chiappe et al. 2002a).

Metacarpal III is completely preserved but is not incorporated into the main carpometacarpal block as in *Mononykus* (Perle et al. 1994). Metacarpal III is much shorter and more slender than metacarpal II. Its proximal articular surface is sub-triangular in outline, predominantly convex and tilted to face somewhat laterally. The ventromedial corner of the proximal surface bears a small depression that probably contributes to the lateral portion of the central facet described above. Most of the shaft of metacarpal III is sub-triangular in cross section. The dorsal margin is sharply ridged along its entire length. The distal end of metacarpal III is strongly compressed transversely, so that the distal end is a plate-like structure with a considerable ventral expansion. The distal end is sharply truncated in lateral view. The dramatic reduction of the distal articular surface to a thin, vertical edge suggests that no phalanges are associated with this digit. In contrast, *Mononykus* and *Shuvuuia* have well-defined condylar distal articulations on the third and fourth metacarpals (Perle et al. 1994; Chiappe et al. 2002b), which are fused to metacarpal II and distal carpals to form the carpometacarpus. In *Shuvuuia*, a complete set of manual digits III and IV are known (Suzuki et al. 2002). These data suggest that *Mononykus* has phalanges on digits III and IV that were not preserved in the holotype.

Manual phalanx II-1 is a large, robust element approximately equal in thickness to the humerus. It has a maximum length/width ratio of about 2.4, compared to a value of 1.5 for the equivalent bone in *Mononykus* (Perle et al. 1994; Chiappe et al. 2002a). Phalanx II-1 is expanded transversely at the proximal end, particularly in the lateral direction. The maximum width/depth ratio is about 1.1, and a moderately developed dorsal process projects from the dorsolateral corner of the proximal articulation. There is also a corresponding, dorsally directed medial process, separated from the lateral one by an intervening depression. The ventral surface of the phalanx bears ridges that extend along the medial and lateral borders. The lateral ridge is much sharper than

the medial one, and the two are separated by a broad axial furrow, a feature unique to alvarezsauroids (Novas 1996; Choiniere 2010; Choiniere et al. 2010). The dorsal surface is narrowest at its distal end, in contrast to the transversely widened distal articular surface seen in *Mononykus* (Perle et al. 1994). However, in *Linhenykus* the ventral part of the distal articulation is considerably wider than the dorsal part. The distal articulation is strongly ginglymoid, with two distinct hemicondyles. Both hemicondyles are narrow transversely and project further ventrally than dorsally, but the medial hemicondyle is narrower than the lateral one. Collateral ligamental fossae are present on both sides. Both are large and shallow, and the lateral fossa is relatively dorsal in position. The distal articular surface extends well onto the dorsal surface of the phalanx, and a distinct extensor fossa is present immediately proximal to the distal articulation. A poorly developed flexor fossa is seen on the ventral surface of the element.

Manual ungual phalanx II-2 is the longest manual element, but is nevertheless proportionally smaller than in other parvicursorines (Chiappe et al. 2002a; Suzuki et al. 2002). It is less than 1.2 times as long as phalanx II-1, but in *Mononykus* the ungual is nearly twice the length of the proximal phalanx (Perle et al. 1994). In *Linhenykus*, phalanx II-2 is robust, and has a stronger curvature than in *Mononykus* (Perle et al. 1994), assuming the proximal articular surface is oriented vertically in both taxa. The transversely broad proximal articular surface is divided into two nearly equal facets by a prominent vertical median ridge. A flexor tubercle is absent, as in all alvarezsaurids in which phalanx II-2 is known (Novas 1996; Longrich and Currie 2008). Instead, the ventral surface is flattened and a distinct but very shallow fossa is present on the ventral surface at a level just distal to the proximal ends of the grooves for the keratinous sheath. From this fossa, a shallow, short and narrow groove extends along the midline of the ventral surface. The lateral and medial sheath grooves are proximally deep and curve ventrally at their proximal ends, each forming a distinct notch in the margin of the proximal part of the ventral surface. These notches are homologous to the closed foramina seen on the ventral surface of phalanx II-2 in *Mononykus* and *Shuvuuia* (Longrich and Currie 2009).

### **Pelvic girdle**

*Ilium.*--The ilium is represented only by the middle part of the left element, including part of the preacetabular process and almost all of the pubic peduncle (Figs. 10A1-A3). The preacetabular process is nearly vertical in orientation, but part of the iliac blade located dorsal to the pubic

peduncle is inclined so that the lateral surface of the blade also faces somewhat dorsally as in other parvicursorines (Xu et al. 2010). In lateral view, the supraacetabular crest extends anteriorly to the level of the pubic peduncle and overhangs the acetabular fossa. The crest is more prominent anteriorly than posteriorly, as in *Mononykus* (Perle et al. 1994, Longrich and Currie 2009). In ventral view, the supraacetabular crest recedes into the anteroventrally-oriented pubic peduncle, which is more ventral and less anterior than is the case in *Mononykus* (Perle et al. 1994). The peduncle is greatly elongated anteroposteriorly and narrow mediolaterally, appearing almost ridge-like in ventral view. A cuppedicus fossa is absent as in other alvarezsaurids (Xu et al. 2010).

### **Figure. 10**

**Pubis.**--Only the proximal part of the left pubis is present (Figs. 10B). As in other alvarezsaurids (Hutchinson and Chiappe 1998), this part of the bone is strongly laterally compressed. In contrast to other parvicursorines (Hutchinson and Chiappe 1998), the proximal articular surface is subtriangular in outline rather than kidney-shaped, but this morphology results at least partly from damage to the anteromedial part of the proximal surface. The articular surface for the ilium appears to be concave, and is much longer than wide. It seems more proximally (as opposed to proximoposteriorly) oriented than is the case in *Mononykus* and *Patagonykus* (Perle et al. 1994; Novas 1997). Its lateral margin is not concave, in contrast to other parvicursorines (Hutchinson and Chiappe 1998). The acetabular fossa of the pubis is slightly inclined ventrolaterally. Its posterolateral corner is built out into a distinct, laterally expanded process. Anteriorly, the pubis differs from those of other parvicursorines in lacking a preacetabular tubercle (Hutchinson and Chiappe 1998). The pubic ischial peduncle is proximodistally long but mediolaterally very thin. The dorsal part of the articular surface for the ischium is transversely wide and markedly concave, whereas the ventral part is strongly compressed and slightly convex. The lateral surface of the proximal part of the pubis is flattened, and overhung by the laterally expanded process at the posterolateral corner of the acetabular fossa. Although there are some morphological differences between the pubis of *Linhenykus* and that of other parvicursorines, the close resemblance of the element in *Linhenykus* and other parvicursorines suggests that *Linhenykus* also had strong opisthopuby as in other parvicursorines (Chiappe et al. 2002b).

### **Hindlimb**

*Femur.*--Both femora are preserved, but neither is complete (Figs. 11A1-A6, B1-B3). The femur is estimated to be slightly more than 70 mm long. A well-developed trochanteric crest appears to be present, but the part of the crest formed by the lesser trochanter is missing. Consequently it is uncertain whether the greater and lesser trochanters are completely fused to each other without any intervening notch, as in other parvicursorines (Chiappe et al. 2002a). The femoral head is medially directed and is perpendicular to both the femoral shaft and the trochanteric crest. The femoral head differs from that of *Mononykus* in being proportionally more stout, and in being separated from the shaft by a slight neck. As in *Mononykus* (Chiappe et al. 2002a), however, the femoral head and trochanteric crest give the proximal end of the femur an L-shaped outline. The proximolateral margin of the femur is smooth and slightly concave, without any trace of a posterior trochanter. The femoral shaft is bowed anteriorly. Three ridges originate from the proximal end, extending along the posterolateral, posteromedial, and anteromedial edges of the femoral shaft. The posterolateral ridge is sharp and extends for more than half of the femoral length, whereas the posteromedial ridge is the weakest of the three. The anteromedial ridge is the most prominent but also the shortest, and its distal end curves posteriorly onto the medial surface of the femur. Lateral to the distal part of the posteromedial ridge lies a distinct 3-mm groove, containing an elongated foramen that is probably homologous to a similarly positioned foramen in *Mononykus* (Perle et al. 1994). No fourth trochanter is present in *Linhenykus* or *Parvicursor*, whereas an incipient fourth trochanter is present in a juvenile specimen of *Shuvuuia* and a weak fourth trochanter is present in all other alvarezsaurids in which the proximal femoral shaft is preserved (Chiappe et al. 2002a; Xu et al. 2010). Posterior and parallel to the anteromedial ridge is a long, wide, and shallow groove. The distal part of this groove widens slightly to form a small fossa. The mediolateral width of the femur increases considerably toward the distal end of the bone. The anterior surface near the distal end is transversely convex over its lateral half and slightly concave over its medial half. The posterior surface of the distal end of the femur forms a large, wide popliteal fossa, bordered on either side by medial and lateral ridges that extend to the distal condyles. The medial ridge is sharper than the lateral. Unlike in *Mononykus*, but resembling the condition seen in *Parvicursor* and *Patagonykus* (Chiappe et al. 2002a), the popliteal fossa is widely open distally. In *Xixianykus*, the popliteal fossa is partially open distally (Xu et al. 2010). The medial condyle is transversely narrow in distal view and sub-triangular in posterior view. The lateral condyle has three projections: an ectocondylar tuber projecting posteriorly, a weak cone-shaped distal projection (present in all alvarezsauroids),

and a weak, ridge-like lateral projection oriented almost anteroposteriorly, possibly an apomorphic feature for *Linhenykus*.

### **Figure. 11**

**Tibia.**--Both tibiae are almost completely preserved (Figs. 11C1-D3). The tibia is about 1.4 times as long as the femur. The proximal end appears to be sub-trapezoidal in proximal view, and is estimated to be only slightly longer anteroposteriorly than transversely. The proximal articular surface is inclined anterolaterally. The cnemial crest extends distally along the tibial shaft for about 14 mm. The fibular condyle is anteroposteriorly long and appears to bear an accessory crest anteriorly, unlike the condition in other parvicursorines (Chiappe et al. 2002a; Xu et al. 2010). As in *Mononykus* and *Parvicursor* (Chiappe et al. 2002a), the medial side of the posterior condyle forms a proximally directed eminence. The fibular and posterior condyles are separated from each other by a relatively deep posterior notch. A fossa is present on the tibial shaft just distal to the notch between the two condyles, and is partly overhung by them. The 18-mm-long fibular crest is narrowly separated from the fibular condyle by a 3mm gap. The crest is sharp, and recedes at both ends. A shallow groove with a distinctly deepened distal end lies posterior and parallel to the fibular crest on the lateral surface of the tibial shaft. The tibial shaft is sub-circular in cross section in the midshaft region. A 20-mm-long weak ridge arises near the midpoint of the tibia's length and runs close to the medial edge of the anterior surface. The distal part of the tibial shaft has a flat posterior surface, whereas the anterior surface has a slight transverse concavity to accommodate the ascending process of the astragalus. A short, distomedially directed crest is present along the distalmost part of the anteromedial margin of the tibia, and a long, sharp ridge separates the anterior and lateral surfaces of the distal end. The lateral portion of the distal end is relatively robust, being subequal in anteroposterior thickness to the medial portion. The distal end of the right tibia has a well-preserved lateral surface, and there is no indication that the fibula reached this part of the tibiotarsus.

**Astragalus and calcaneum.**--The astragalus-calcaneum complex is represented only by pieces of bone attached to the distal ends of both tibiae (Figs. 11C1, D1 and E). The astragalus-calcaneum complex is tightly articulated with the tibia, and the left tibiotarsus even shows co-ossification among the three elements. The main body of the astragalus is poorly preserved in both the left and right hindlimbs. As in *Mononykus* (Chiappe et al. 2002a), the laminar ascending process is approximately L-shaped in anterior view due to a strong indentation on the medial side. The

ascending process arises only from the lateral half of the body of the astragalus, so that the medial edge of the ascending process is close to the midline of the tibial shaft. A shallow anterior fossa is present at the base of the ascending process.

*Pes.*--The preserved pedal elements include: nearly complete left metatarsus; distal end of right metatarsal IV, and other probable right metatarsal fragments; left pedal phalanges I-1 and I-2; left pedal phalanx II-1, partial II-2, and complete II-3; partial left pedal phalanges III-1 and III-3, complete III-2, and complete left pedal ungual III-4; left pedal phalanges IV-1, IV-2, IV-3 and partial IV-4 in articulation (Fig. 12).

### **Figure. 12**

The metatarsus is 73 mm long, and its transverse width is less than 5 mm in the midshaft region. As in other parvicursorines (Chiappe et al. 2002a; Longrich and Currie 2009; Xu et al. 2010), the metatarsus is longer than the femur, and exhibits a specialized arctometatarsalian condition in which metatarsal III terminates well distal to the proximal end of the metatarsus as in other parvicursorines (Longrich and Currie 2009, Turner et al. 2009, Xu et al. 2010). In less specialized arctometatarsal taxa, metatarsal III normally extends right to the proximal end of the metatarsus in an attenuated form (Hutchinson and Padian 1997).

Metatarsal II is straight for most of its length, although the proximal and distal ends both have a strong medial curvature. The proximal end of metatarsal II appears to have a sub-triangular outline, though its lateral portion is missing in the only preserved example of this element. Relative to the midshaft, the proximal end is strongly expanded both dorsally and laterally. Just 7 mm away from the proximal end is a short groove along the dorsomedial margin. The shaft is deeper dorsoventrally than wide transversely for its entire length, although the discrepancy is reduced in the distal third of the shaft. A weak crest is present along the ventromedial margin over about the middle third of the shaft. A slight collateral ligamental pit appears to be present on the medial side of the distal end of the metatarsal.

Metatarsal III is visible over about the distal two-fifths of the metatarsus in dorsal view and over less than the distal one-fifth in ventral view. Proximally, this metatarsal is wedge-shaped, fitting tightly between metatarsals II and IV. From the sharply pointed proximal end of metatarsal III, the dorsal surface of the shaft rapidly widens and indeed becomes broader than the other metatarsals in dorsal view, but subsequently undergoes a slight constriction and remains narrow for approximately the distal three-fifths of its length. The dorsal surface proximal to the constriction is



slightly concave transversely, a feature also seen in other Asian parvicursorines (Longrich and Currie 2009). Ventrally the shaft forms a weak longitudinal ridge extending toward the distal end. As preserved, the distal portion of metatarsal III curves considerably ventrally, as does that of metatarsal IV. The distal end is considerably wider transversely than those of metatarsals II and IV. The articular surface is not ginglymoid, though oblique hemicondylar ridges are weakly developed on the ventral surface. The distal articular surface extends some distance proximally onto the dorsal surface of the shaft. Large and deep collateral ligamental fossae are present on the medial and lateral sides of the distal end of the metatarsal.

Metatarsal IV is only slightly longer than metatarsal II and is closely appressed to the latter for most of its length, although in the distalmost part of the metatarsus the two are separated by metatarsal III. Metatarsal IV is much deeper dorsoventrally than wide transversely for most of its length, and its distal end appears to curve laterally. Metatarsal IV is transversely wider than metatarsal II over the proximal half of the metatarsus, but narrower over the distal half. A weak crest runs along the proximal half of the ventrolateral margin. The distal end of metatarsal IV is slightly expanded dorsally and strongly expanded ventrally. The distal articulation is non-ginglymoid. The dorsal exposure of the articular surface is strongly skewed towards the lateral side of the metatarsal. On the ventral surface of the distal end two prominent ridge-like hemicondyles are developed, the lateral hemicondyle being more ventrally prominent than the medial. There is no collateral ligamental pit on the lateral side of the distal end of the metatarsal.

The pedal phalanges are relatively long and slender compared to those of *Mononykus* (Perle et al. 1994). All of the non-ungual phalanges are sub-rectangular in cross section, and have strongly ginglymoid distal ends with hemicondyles that are of considerable extent both dorsoventrally and proximodistally. Collateral ligamental fossae are well developed on most of the non-ungual phalanges, although the pits on the penultimate phalanges are shallow. The proximal phalanges have distinct extensor fossae immediately proximal to their distal articular surfaces, and less distinct fossae are also present on the intermediate phalanges.

Pedal phalanx I-1 is small. Its proximal articular surface is nearly flat and inclined to face slightly dorsally. The dorsal and ventral margins do not form prominent lips, suggesting that the distal end of metatarsal I is non-ginglymoid. The distal hemicondyles of phalanx I-1 are more prominent dorsally than ventrally, and the medial hemicondyle is larger than the lateral. A shallow collateral ligamental fossa is located ventrally on the medial surface of the distal articulation,

whereas the lateral surface is flat. Phalanx II-1 is much deeper dorsoventrally at the proximal end than at the distal end. Distally the phalanx bears not only a distinct extensor fossa, but also a prominent flexor fossa bounded laterally and medially by significant proximal extensions of the hemicondyles. The ventral lip of the proximal end of phalanx II-2 is asymmetrical, with its tip medially positioned. Phalanx III-1 has a strongly expanded proximal end, but the shaft narrows significantly as it passes distally. Phalanx IV-1 is a relatively robust element. Its proximal end is deeply notched on the ventral side, with a long and robust medial process and a short, transversely thin lateral process, as in other parvicursorines (Longrich and Currie 2009). The lateral collateral ligamental fossa is shallow and located centrally on the lateral surface of the distal end of the phalanx, whereas the medial fossa appears deep.

The pedal ungual phalanges are moderately curved and laterally compressed, each having a sub-elliptical cross section. The preserved examples all lack flexor tubercles, and their arcuate sheath grooves are relatively weak. Phalanx I-2 is asymmetrical, having a relatively flat lateral margin but a more convex medial margin.

### **Morphological evolution**

A numerical phylogenetic analysis produced two most parsimonious trees, each with a tree length of 103 steps, a CI of 0.79, and a RI of 0.86 (Figs. 13A, B), and recovers *Linhenykus* as a basal parvicursorine alvarezsauroid (Xu et al. 2011d). The optimized synapomorphies for the Alvarezsauroidea and more exclusive clades are listed in Appendix 1.

The synapomorphies shared with other parvicursorines include dorsal vertebrae opisthocoelous and without hyposphene-hypantrum articulations, dorsal parapophyses elevated to level of diapophyses, dorsal infradiapophyseal fossae hypertrophied, posterior sacral vertebrae with hypertrophied ventral keels, anterior caudal vertebrae with anteriorly displaced transverse processes, metacarpal II that is mediolaterally wider than proximodistally long and dorsoventrally shallow, bears two articular facets on the proximal surface, and lacks collateral ligamental fossae, manual ungual II with ventral axial groove and without flexor tubercle, tibial distal end with lateral malleolus anteroposteriorly expanded, astragalar ascending process L-shaped, and specialized arctometatarsalian condition with metatarsal III shorter than metatarsals II and IV. Other possible parvicursorine synapomorphies seen in *Linhenykus* include posterior dorsal vertebrae with small and posterodorsally oriented neural spines, biconvex vertebra near posterior end of dorsal

series, keeled and boatlike sternum with median groove along midline, manual phalanx II-2 longer than II-1, supracetabular crest of ilium more prominent anteriorly than posteriorly, metatarsus longer than femur, metatarsals II and IV subequal in length, and pedal digit III more slender than digits II and IV.

These synapomorphies are mostly related to the appendicular skeleton, which is unsurprising given that *Shuvuuia* is the only alvarezsaurid in which the skull is well-known (Chiappe et al. 2002a). Indeed, parvicursorines apparently differ from other non-avian theropods in having highly specialized forelimbs and hindlimbs (Chiappe et al. 2002a). While their forelimb morphology has received much attention (Zhou 1995; Senter 2005; Longrich and Currie 2009), little attention has so far been paid to their hindlimbs, although hindlimb morphology has been extensively studied in other theropod groups (Gatesy 1991; Hutchinson 2001; Carrano and Hutchinson 2002).

The highly modified hindlimbs of parvicursorines have been interpreted as an adaptation for rapid running (Xu et al. 2010). One commonly used indicator of cursoriality is the length of the crural segment of the hindlimb relative to that of the femoral segment, though this is probably more effective in promoting energy efficiency during running than in permitting a high maximum speed. Previous analyses have shown that derived theropods possess relatively greater tibia/femur length ratios than primitive ones, and this evolutionary trend continues into the Aves (Gatesy 1991; Jones et al. 2000; Christiansen and Bonde 2002). However, many theropod groups display an opposite trend during their evolutionary history: basal members of these theropod groups (for example, the Ceratosauria, the Tyrannosauroidae, the Therizinosauroidae, the Oviraptorosauria, the Troodontidae, and the Dromaeosauridae) have relatively longer distal segments of the hindlimb than derived members of each group. Alvarezsauroidae and Aves are exceptional among the major theropod groups in elongating the crural segment of the hindlimb in their evolutionary history, which is probably related to a size-decrease trend within these two groups. *Linhenykus* has a tibia/femur length ratio of about 1.40, similar to other parvicursorines but significantly greater than in basal alvarezsauroids and most other non-avian theropods (Gatesy 1991; Jones et al. 2000; Christiansen and Bonde 2002). In Aves, the evolutionary pattern was more complex: significant distal limb elongation took place, but was preceded by significant distal limb shortening close to the base of the Aves (Hu et al. 2010). We interpret this temporary shortening trend as resulting from either a substantial improvement in flight capability (and thus decreased reliance on the hind limb for

primary locomotion) or a shift toward an arboreal life style (a very long crus and foot might be awkward in climbing, and reducing the overall mass of the hind limb would be helpful to a flier), and the distal limb elongation in more derived birds as resulting from a shift toward avian-style locomotion in which movements of the lower hindlimb segments predominated in running and particularly in walking (Jones et al. 2000). In derived alvarezsauroids, pronounced elongation of the tibiotarsus relative to the femur is more likely to indicate increased cursorial capability. Given that parvicursorines have higher tibia/femur ratios than most other non-avian theropods, they are probably among the most capable cursors within this evolutionary grade (Xu et al. 2010). Further indicators of cursorial specialization include the extremely elongate metatarsus (longer than the femur), specialized arctometatarsalian pes, and proportionally short and robust pedal phalanges of alvarezsaurids. Some of these features are also known in ornithomimosaurids (Makovicky et al. 2004), another non-avian theropod group regarded as highly cursorial. In less specialized cursorial non-avian theropods such as troodontids, the metatarsus is shorter and the pedal phalanges are more slender.

### **Historical biogeography of the Alvarezsauroidea**

The historical biogeography of alvarezsauroids has received considerable attention during the past two decades. Initially, some authors (e.g. Bonaparte 1991) suggested that *Alvarezsaurus calvoi* represented a lineage of Cretaceous theropods that were endemic to Gondwana, perhaps converging to some degree on the Laurasian ornithomimosaurids (Barsbold and Osmolska 1990; Novas 1997). However, this idea was rapidly overturned as a result of the discovery of first East Asian and then North American alvarezsauroids (Novas 1997; Hutchinson and Chiappe 1998). This wider geographic distribution has been interpreted in two ways: pre-Aptian vicariance versus Late Cretaceous dispersals. The vicariance model was proposed by Novas (1996), who suggested that alvarezsaurids probably originated during or before the Early Cretaceous and therefore spread across Pangaea before geographic barriers separated Laurasia and Gondwana from the Aptian onwards. In contrast, the dispersal hypothesis envisages alvarezsaurids originating in South America initially, followed by at least one dispersal event into North America, followed in turn by at least one dispersal event from the latter into East Asia (Martinelli and Vera 2007; Longrich and Currie 2009). This hypothesis is based on the observations that: (1) the most basal alvarezsaurids come from South America whereas the most derived ones occur in East Asia (Martinelli and Vera

2007; Longrich and Currie 2009); and (2) some palaeogeographic and biogeographic evidence support faunal exchanges between North and South America (Bonaparte and Kielan-Jaworowska 1987; Lucas and Hunt 1989; Gayet et al. 1992; Sullivan and Lucas 2000), and between North America and East Asia (Russell 1993; Le Loeuff 1997; Hutchinson and Chiappe 1998; Sereno 1999), across landbridges that formed during the Late Cretaceous.

There is, however, a third interpretation of the observed distributions of alvarezsaurids: that is, the ‘null’ biogeographic hypothesis. The latter states that there is no detectable biogeographic pattern because the data are inadequate or because genuine distribution signals have been obscured by missing data. The null biogeographic hypothesis should be rejected (via analytical and statistical approaches) before we accept the possibility of a genuine biogeographic pattern (Page 1991; Upchurch et al. 2002; Sanmartin and Ronquist 2004; Upchurch 2008), but no previous study has attempted this for the alvarezsaurids. Below, we use the new alvarezsauroid phylogeny presented in Xu et al. (2011) to test competing biogeographic hypotheses utilizing a cladistic biogeographic method and statistical evaluation based on randomization tests.

*Methods.*—Ronquist (1998) and Sanmartin and Ronquist (2004) proposed the cladistic biogeographic method known as Treefitter. In this approach, each type of biogeographic event is assigned a cost. The default costs in Treefitter are vicariance = 0, sympatry = 0, extinction = 1, and dispersal = 2. However the investigator can alter these costs. For example, setting vicariance = -1 and the three other event types = 0, produces a ‘maximum codivergence’ analysis analogous to that implemented in the programs Component (Page 1993, 1995), as has been applied to dinosaurs (Upchurch et al. 2002; Butler et al. 2006) and crocodyliforms (Turner 2004). Treefitter uses phylogenetic topologies and information on the geographic ranges of the terminal taxa to generate the most parsimonious biogeographic reconstruction (i.e. the biogeographic history with the lowest overall event cost, that explains the distributions of the taxa).

It is conceivable that taxon distributions are random with respect to phylogeny (the null hypothesis): therefore, this possibility must be tested before the biogeographic reconstruction can be legitimately interpreted as a set of genuine evolutionary events. To test the null hypothesis, the phylogenetic topology, or the positions of terminal taxa with respect to that topology, are randomized and the event cost calculated for these random data. This process is repeated thousands of times, so that a population of randomized results is generated. If the event cost required by the original (unrandomized) data is less than the event costs of 95% of the randomized data sets, then

the null hypothesis can be rejected with a  $p$ -value of  $< 0.05$ . Treefitter can also reconstruct the frequencies of each of the four types of biogeographic event, and randomization tests can again be used to determine whether these frequencies depart significantly from values expected from random data sets (Ronquist 1998, Sanmartin and Ronquist 2004).

*Analyses and results.*—The phylogenetic analysis of Xu *et al.* (2011) produced a fully resolved cladogram apart from the trichotomy between *Achillesaurus*, *Alvarezsaurus* and the remaining clade of more derived alvarezsaurids. For the purposes of biogeographic analysis, this gives two topologies that should be explored: (1) *Achillesaurus* and *Alvarezsaurus* are sister taxa (Fig. 13A); and (2) *Alvarezsaurus* and the remaining derived alvarezsaurid clade are sister taxa (i.e. *Achillesaurus* is the most basal taxon) (Fig. 13B). The third possibility, in which *Achillesaurus* and derived alvarezsaurids are sister-taxa to the exclusion of *Alvarezsaurus*, is biogeographically equivalent to tree 2 in Figure 13 because both *Achillesaurus* and *Alvarezsaurus* occur in South America. The taxa in Trees 1 and 2 have been assigned to three geographic areas (A = Asia; N = North America; S = South America) to create the Treefitter data sets shown in Appendix 1. These data sets have been analyzed using the exhaustive search option under the default and maximum codivergence cost regimes in Treefitter 1.2b (Ronquist 1998). For each analysis, randomization tests were carried out using 10,000 replicates in which the tree topology was perturbed each time. In addition, the frequencies of the four types of biogeographic event have been calculated and their statistical significance evaluated using 10,000 random replicates.

### Figure. 13

The results of these analyses are summarized in Tables 1 and 2, and indicate the following:

- Each analysis produced two optimal area cladograms (OACs), and across all analyses all three possible relationships between Asia, North America and South America are represented in these OACs (Table 1). Restricting consideration purely to OACs that are statistically significant, however, allows rejection of the topology (Asia (North America, South America)).
- The choice of cost regime strongly affects the statistical support for the reconstructions. Under the default cost, data set 2 passes the randomization test and data set 1 fails narrowly (Table 1). However, under the maximum codivergence cost regime, both data sets produce statistically insignificant reconstructions (Table 1).

- The alternative positions of the South American alvarezsaurids near the base of the phylogeny (see Trees 1 and 2 in Figure 13) have some effect on biogeographic reconstructions. In particular, data set 2 produces more statistically significant event frequency results than does data set 1 (Table 2).
- The biogeographic reconstructions produced under the default cost regime have low p-values, which suggest that the null hypothesis can be rejected. However, examination of the event frequencies in Table 2 demonstrates that dispersal does not occur more or less often than expected, and in some instances vicariance and extinction occur less often than expected, in random data. Thus, it seems that these biogeographic reconstructions are largely statistically significant because of their higher than expected frequencies of sympatric events.

*Discussion.*—The statistically significant optimal area cladograms produced by the Treefitter analyses are compatible with both the pre-Aptian vicariance and Late Cretaceous dispersal hypotheses outlined above. For example, the topology (South America, (Asia, North America)) could have arisen as a result of the formation of geographic barriers first between Laurasia and Gondwana, and then between Asia and North America. The same area cladogram topology would also occur if alvarezsaurids originated in South America, and then dispersed to Asia, or North America, or Asia North America (although it should be noted that none of the optimal reconstructions explain the geographic distributions via dispersal alone, or via dispersal, sympatry and extinction without vicariance). The optimal area cladogram topology is also compatible with reconstructions that mix vicariance and dispersal events (e.g. see the event frequencies for data set 2 under default costs, Table 2). Thus, it is clear that the OACs by themselves, do not allow a convincing rejection of any of the biogeographic histories proposed previously. Moreover, these results identify equally valid, but hitherto unconsidered histories involving a more complex mix of vicariance, regional extinction and dispersal.

The event frequencies are somewhat more informative than the optimal area cladograms: Table 2 indicates that the frequencies of vicariance, extinction and dispersal are no higher than would be expected from random data, irrespective of which cost regime is applied or which data set is analyzed. The only statistically significant results relate to higher than expected levels of sympatry in both data sets, and lower than expected rates of vicariance and extinction in data set 2. Thus, there is no statistical support for either the pre-Aptian vicariance or Late Cretaceous dispersal

hypotheses proposed by other workers. Nevertheless, the geographic distributions of alvarezsaurids are not entirely random with respect to their phylogeny because there appears to be more sympatry than expected from random data.

The results produced by these analyses should be interpreted with caution. First, as discussed by Upchurch et al. (2002) there are numerous reasons why a cladistic biogeographic data set might fail to produce statistically significant results. In particular, it is important to recognize that statistical failure means that there is an absence of evidence for one or more biogeographic events, not evidence of absence. Thus, alvarezsaurid distributions may actually have been shaped by vicariance and/or dispersal, but statistically robust evidence that demonstrates this is lacking at present. A related point is that cladistic biogeographic analyses cannot distinguish between true sympatry (speciation within a geographic area resulting from ecological or behavioral partitioning) and ‘within area’ allopatry (i.e. vicariance that occurs as a result of barrier formation within the geographic area). Thus, some or all of the sympatric events, such as the divergences between derived Asian alvarezsaurid taxa, might actually represent vicariance between different parts of Asia.

Second, our results suggest that the biogeographic history of alvarezsaurids is likely to be somewhat more complex than previously realized. This is supported by the recent discovery of *Heptasterornis*, a derived alvarezsaurid from the Maastrichtian of Romania (Naish and Dyke 2004). This taxon shares some derived character states of the femur with advanced Asian alvarezsaurids, hinting at a close phylogenetic relationship (Xu et al. 2011d). It is interesting to note that *Heptasterornis* potentially clusters within a monophyletic Laurasian clade that also includes North American and Asian forms. This pattern could have been produced by a pre-Aptian vicariance event, as proposed by Novas (1996). Alternatively, regression of the Turgai sea during the Aptian-Albian might have produced a temporary landbridge between Asia and Europe (Upchurch et al. 2002), and therefore have enabled the ancestor of *Heptasterornis* to disperse from the former area to the latter at this time. Unfortunately, *Heptasterornis* is known from very fragmentary remains, which do not permit its phylogenetic position to be established precisely (Xu et al. 2011c; Dyke and Naish 2011). Thus, discoveries of additional alvarezsaurid material from the Late Cretaceous of Europe and Central Asia, and indeed Early Cretaceous specimens from other continents, will be needed before these competing scenarios can be tested more rigorously.



Finally, the current data set is very small (12 ingroup alvarezsaurids) compared to those that have successfully recovered vicariance and dispersal patterns using cladistic methods (e.g. 150 dinosaurian genera (Upchurch et al. 2002); 29 crocodyliform genera (Turner 2004); over 1000 extant species (Sanmartin and Ronquist 2004). There are many Late Cretaceous dinosaur groups with close relatives distributed across both North America and Asia (e.g. ornithomimosaurs, tyrannosaurs, ceratopsids (Weishampel et al. 2004)) and some of these also have representatives in South America (e.g. dromaeosaurids (Makovicky et al. 2005)). It is conceivable that a larger data set will provide evidence of a consistent biogeographic pattern repeated across many of these clades, providing statistically significant support for vicariance and/or dispersal events.

## **Conclusion**

*Linhenykus* is an advanced alvarezsaurid from the Late Cretaceous of Asia, and is referable to the Parvicursorinae. This new genus provides the first example of monodactyly among dinosaurs. Clearly, as well as the major trends in manus evolution that occurred during the theropod-bird transition, there must have been much ‘experimentation’ with hand structure in several of the ‘side branches’ such as tyrannosauroids and alvarezsauroids.

The study of alvarezsauroid historical biogeography serves as an example of the dangers associated with interpreting macroevolutionary patterns based on literal readings of the fossil record. Several workers have generated scenarios to explain the observed geographic and stratigraphic ranges of alvarezsauroids without first ruling out the possibility that these distributions are effectively random because of the paucity of the fossil record. Cladistic biogeographic analysis indicates that there is some signal in the alvarezsauroid record, but this relates to elevated levels of sympatry (or ‘within continent vicariance’) rather than evidence for dispersal or continent-level vicariance. Inferences of biogeographic history derived from small palaeobiological datasets should be treated with extreme caution, especially when the null biogeographic hypothesis has not been rejected. In the future, discovery of new fossils will play a vital role in improving our understanding of the biogeographic history of alvarezsauroids, but the application of appropriate analytical methods will be equally important.

## **Acknowledgments**

We thank Wang Jianming, Liu Jinsheng, Li Zhiqian, and Zhao Xinquan for coordinating the project, Wang Haijun for assistance in the field and Yu Tao and Ding Xiaoqin for preparing the specimen. This work was supported by the National Natural Science Foundation of China, the Department of Land and Resources, Inner Mongolia, China, the Gloyne Outdoor Geological Research Fund of the Geological Society of London, National Science Foundation Office of International Science and Engineering grant 0812234, the Jurassic Foundation, and the Robert Weintraub Program for Systematics and Evolution at the George Washington University.

## References

- Barsbold, R. and Osmólska, H. 1990. Ornithomimosauria. *In*: D.B. Weishampel, P. Dodson, and H. Osmólska (eds.), *The Dinosauria (First edition)*, 225-248. University of California Press, Berkeley.
- Bonaparte, J.F. 1991. The vertebrate fossils of the Rio Colorado Formation, from the city of Neuquén and surrounding areas, Upper Cretaceous, Argentina (Translated from Spanish). *Paleontología* 4 (3): 17-123.
- Bonaparte, J.F. and Kielan-Jaworowska, K. 1987. Late Cretaceous dinosaur and mammal faunas of Laurasia and Gondwana. *In*: P.J. Currie, and E.H. Koster (eds.), *Fourth Symposium on Mesozoic Terrestrial ecosystems, Short Papers.* , 24-29. Occasional Papers of the Tyrell Museum of Palaeontology, Drumheller.
- Butler, R.J., Upchurch, P., Norman, D.B., and Parish, J.C. 2006. A biogeographical analysis of the ornithischian dinosaurs. Pp. 13-16. *In* P.M. Barrett, and S.E. Evans, eds. Ninth International Symposium on Mesozoic Terrestrial Ecosystems and Biota. The Natural History Museum, London.
- Carrano, M.T. and Hutchinson, J.R. 2002. Pelvic and hindlimb musculature of *Tyrannosaurus rex* (Dinosauria: Theropoda). *Journal of Morphology* 253 (3): 207-228.
- Chatterjee, S. 1998. Counting the fingers of birds and dinosaurs. *Science* 280: 355a.
- Chiappe, L., Norell, M.A., and Clark, J.A. 2002a. The Cretaceous short-armed Alvarezsauridae: *Mononykus* and its kin. *In*: L.M. Chiappe, and L.M. Witmer (eds.), *Mesozoic birds: above the heads of dinosaurs*, 87-120. University of California Press, Berkeley.
- Chiappe, L.M., Norell, M.A., and Clark, J.M. 1998. The skull of a relative of the stem-group bird *Mononykus*. *Nature* 392: 275-282.

- Chiappe, L.M., Norell, M.A., and Clark, J.M. 2002b. The Cretaceous, short-armed Alvarezsauridae: *Mononykus* and its kin. In: L.M. Chiappe, and L.M. Witmer (eds.), *Mesozoic birds: above the heads of dinosaurs*, 87-120. University of California Press, Berkeley.
- Choiniere, J. 2010. *Anatomy and systematics of coelurosaurian theropods from the Late Jurassic of Xinjiang, China, with comments on forelimb evolution in Theropoda* 1015 pp., George Washington University, Washington DC.
- Choiniere, J.N., Xu, X., Clark, J.M., Forster, C.A., Guo, Y., and Han, F.L. 2010. A basal alvarezsauroid theropod from the early Late Jurassic of Xinjiang, China. *Science* 327: 571-574.
- Christiansen, P. and Bonde, N. 2002. Limb proportions and avian terrestrial locomotion. *Journal of Ornithology* 143: 356-371.
- Christiansen, P. and Fariña, R.A. 2004. Mass prediction in theropod dinosaurs. *Historical Biology* 16: 85-92.
- Chure, D.J. 2001. The wrist of *Allosaurus* (Saurischia: Theropoda), with observations on the carpus in theropods. In: J.A. Gauthier, and L.F. Gall (eds.), *New perspectives on the origin and early evolution of birds*, 122-130. Yale University Press, New Haven.
- Dyke, G. and Naish, D. 2011. What about European alvarezsauroids. *Proceedings of the National Academy of Sciences of the United States of America* 108 (22): E147.
- Gatesy, S.M. 1991. Hind limb scaling in birds and other theropods: implications for terrestrial locomotion. *Journal of Morphology* 209: 83-96.
- Gauthier, J. 1986. Saurischian monophyly and the origin of birds. *Memoirs of the California Academy of Sciences* 8: 1-55.
- Gayet, M., Rage, J.-C., Sempere, T., and Gagnier, P.Y. 1992. Modalités des échanges de vertébrés continentaux entre l'Amérique du Nord et l'Amérique du Sud au Crétacé supérieur et au Paléocène. *Bulletin De La Societe Geologique De France* 163: 761-791.
- Hu, D.-Y., Li, L., Hou, L.-H., and Xu, X. 2010. A new sapeornithid bird from China and Its implication for early avian evolution. *Acta Geologica Sinica* 84: 472-482.
- Hutchinson John, R. 2001. *The evolution of hindlimb anatomy and function in theropod dinosaurs*. 357 pp., University of California, Berkeley.
- Hutchinson, J.R. and Chiappe, L.M. 1998. The first known alvarezsaurid (Theropoda: Aves) from North America. *Journal of Vertebrate Paleontology* 18 (3): 447-450.

- Hutchinson, J.R. and Padian, K. 1997. Arctometatarsalia. *In*: P.J. Currie, and K. Padian (eds.), *Encyclopedia of dinosaurs*, 24-27. Academic Press, San Diego.
- Irmis, R.B. 2007. Axial skeletal ontogeny in the Parasuchia (Archosauria: Pseudosuchia) and its implications for ontogenetic determination in Archosaurs. *Journal of Vertebrate Paleontology* 27 (2): 350-361.
- Jerzykiewicz, T., Currie, P.J., Eberth, D.A., Johnston, P.A., Koster, E.H., and Zheng, J.-J. 1993. Djadokhta Formation correlative strata in Chinese Inner Mongolia: an overview of the stratigraphy, sedimentary geology, and paleontology and comparisons with the type locality in the pre-Altai Gobi. *Canadian Journal of Earth Sciences* 30: 2180-2190.
- Jones, T.D., Farlow, J.O., Ruben, J.A., Henderson, D.M., and Hillenius, W.J. 2000. Cursoriality in bipedal archosaurs. *Nature* 406 (6797): 716-718.
- Karhu, A.A. and Rautian, A.S. 1996. A new family of Maniraptora (Dinosauria: Saurischia) from the Late Cretaceous of Mongolia. *Paleontological Journal* 30 (5): 583-592.
- Kessler, E., Grigorescu, D., and Csiki, Z. 2005. *Elopteryx* revisited – a new bird-like specimen from the Maastrichtian of the Hateg Basin (Romania). *Acta Palaeontologica Romaniae* 5: 249-258.
- Kundrát, M., Seichert, V., Russell, A.P., and Smetana, K. 2002. Pentadactyl pattern of the avian wing autopodium and pyramid reduction hypothesis. *Journal of Experimental Zoology (Mol Dev Evol)* 294: 152-159.
- Le Loeuff, J. 1997. Biogeography. *In*: P.J. Currie, and K. Padian (eds.), *Encyclopedia of dinosaurs*, 51-56. Academic Press, San Diego.
- Longrich, N.R. and Currie, P.J. 2008. *Albertonykus borealis*, a new alvarezsaur (Dinosauria: Theropoda) from the Early Maastrichtian of Alberta, Canada: implications for systematics and ecology of the Alvarezsauridae. *Cretaceous Research* 30 (1): 239-252.
- Longrich, N.R. and Currie, P.J. 2009. *Albertonykus borealis*, a new alvarezsaur (Dinosauria: Theropoda) from the Early Maastrichtian of Alberta, Canada: implications for the systematics and ecology of the Alvarezsauridae. *Cretaceous Research* 30: 239-252.
- Lucas, S.G. and Hunt, A.P. 1989. *Alamosaurus* and the sauropod hiatus in the Cretaceous of the North American western interior. *Geological Society of America Special Paper* 238: 75-85.
- Makovicky, P.J., Apesteguía, S., and Agnolín, F.L. 2005. The earliest dromaeosaurid theropod from South America *Nature* 437: 1007-1011.

- Makovicky, P.J., Kobayashi, Y., and Currie, P.J. 2004. Ornithomimosauria. *In*: D.B. Weishampel, P. Dodson, and H. Osmolska (eds.), *The Dinosauria (second edition)*, 137-150. University of California Press, Berkeley.
- Martinelli, A.G. and Vera, E. 2007. *Achillesaurus manazzoni*, a new alvarezsaurid theropod (Dinosauria) from the Late Cretaceous Bajo de la Carpa Formation, Río Negro Province, Argentina. *Zootaxa* 1582: 1-17.
- Naish, D. and Dyke, G. 2004. *Heptasteornis* was no ornithomimid, troodontid, dromaeosaurid or owl: the first alvarezsaurid (Dinosauria: Theropoda) from Europe. *Neues Jahrbuch für Geologie und Paläontologie Monatshefte* 7: 385-401.
- Novas, F.E. 1996. Alvarezsauridae, Cretaceous basal birds from Patagonia and Mongolia. *Memoirs of the Queensland Museum* 39 (3): 675-702.
- Novas, F.E. 1997. Anatomy of *Patagonykus puertai* (Theropoda, Maniraptora, Alvarezsauridae) from the Late Cretaceous of Patagonia. *Journal of Vertebrate Paleontology* 17 (1): 137-166.
- Page, R.D.M. 1991. Random dendrograms and null hypotheses in cladistic biogeography. *Systematic Zoology* 40: 54-62.
- Page, R.D.M. 1993. Component vers. 2.0 The Natural History Museum, London.
- Page, R.D.M. 1995. TreeMap for Windows vers. 1.0a
- Perle, A., Chiappe, L.M., Barsbold, R., Clark, J.M., and Norell, M. 1994. Skeletal morphology of *Mononykus olecranus* (Theropoda: Avialae) from the Late Cretaceous of Mongolia. *American Museum Novitates* 3105: 1-29.
- Perle, A., Norell, M.A., Chiappe, L., and Clark, J.M. 1993. Flightless bird from the Cretaceous of Mongolia. *Nature* 362: 623-626.
- Ronquist, F. 1998. Three-dimensional cost-matrix optimization and maximum cospeciation. *Cladistics* 14 (2): 167-172
- Russell, D.A. 1993. The role of Central Asia in dinosaurian biogeography. *Canadian Journal of Earth Sciences* 30: 2002-2012.
- Salgado, L., Coria, R.A., Arcucci, A.B., and Chiappe, L.M. 2009. Remains of Alvarezsauridae (Theropoda, Coelurosauria) in the Allen Formation (Campanian-Maastrichtian), in Salitral Ojo de Agua, Río Negro Province, Argentina. *Andean Geology* 36 (1): 67-80.
- Sanmartin, I. and Ronquist, F. 2004. Southern Hemisphere biogeography inferred by event-based models: plant versus animal patterns. *Systematic Biology* 53: 216-243.

- Senter, P. 2005. Function in the stunted forelimbs of *Mononykus olecranus* (Theropoda), a dinosaurian anteater. *Paleobiology* 31: 373-381.
- Sereno, P.C. 1999. Dinosaurian biogeography; vicariance, dispersal and regional extinction. *National Science Museum Monographs* 15: 249-257.
- Sullivan, R.M. and Lucas, S.G. 2000. *Alamosaurus* (Dinosauria: Sauropoda) from the late Campanian of New Mexico and its significance. *Journal of Vertebrate Paleontology* 20 (2): 400-403.
- Suzuki, S., Chiappe, L.M., Dyke, G.J., Watabe, M., Barsbold, R., and Tsogtbataar, K. 2002. A new specimen of *Shuvuuia deserti* Chiappe et al., 1998, from the Mongolian Late Cretaceous with a discussion of the relationships of alvarezsaurids to other theropod dinosaurs. *Contributions in Science* 494: 1-18.
- Tamura, K., Nomura, N., Seki, R., Yonei-Tamura, S., and Yokoyama, H. 2011. Embryological evidence identifies wing digits in birds as digits 1, 2, and 3. *Science* 331: 753-757.
- Turner, A.H. 2004. Crocodyliform biogeography during the Cretaceous: evidence of Gondwanan vicariance. *Proceedings of The Royal Society of London Series B* 271 (1552): 2003-2009.
- Turner, A.H., Nesbitt, S.J., and Norell, M.A. 2009. A large alvarezsaurid from the Late Cretaceous of Mongolia. *American Museum Novitates* 3648: 1-14.
- Upchurch, P. 2008. Gondwanan break-up – legacies of a lost world? *Trends in Ecology and Evolution* 23 (4): 229-236.
- Upchurch, P., Hunn, C.A., and Norman, D.B. 2002. An analysis of dinosaurian biogeography: evidence for the existence of vicariance and dispersal patterns caused by geological events. *Proceedings of the Royal Society of London Series B-Biological Sciences* 269 (1491): 613-621.
- Vargas, A.O. and Fallon, J.F. 2005. Birds have dinosaur wings: the molecular evidence. *Journal of Experimental Zoology (Mol Dev Evol)* 304B: 86-90.
- Vargas, A.O., Kohlsdorf, T., Fallon, J.F., Brooks, J.V., and Wagner, J.P. 2008. The evolution of HoxD-11 expression in the bird wing: insights from *Alligator mississippiensis*. *PLoS ONE* 3: e3325.
- Wagner, G.P. and Gauthier, J.A. 1999. 1,2,3 = 2,3,4: a solution to the problem of the homology of the digits in the avian hand. *Proceedings of National Academy of Sciences, USA* 96: 5111-5116.

- Weishampel, D.B., Barrett, P.M., Coria, R.A., Loeuff, J.L., Xu, X., Zhao, X.J., Sahni, A., Gomani, E., and Noto, C.R. 2004. Dinosaur distribution. *In*: D.B. Weishampel, P. Dodson, and H. Osmólska (eds.), *The Dinosauria (second edition)*. University of California Press, Berkeley.
- Wilson, J.A. 1999. A nomenclature for vertebral laminae in sauropods and other saurischian dinosaurs. *Journal of Vertebrate Paleontology* 19 (4): 639-653.
- Xu, X., Clark, J.M., Mo, J.-Y., Choiniere, J., Forster, C.A., Erickson, G.M., Hone, D.W.E., Sullivan, C., Eberth, D.A., Nesbitt, S., Zhao, Q., Hernandez, R., Jia, C.K., Han, F.-L., and Guo, Y. 2009. A Jurassic ceratosaur from China helps clarify avian digit homologies. *Nature* 459: 940-944.
- Xu, X., Sullivan, C., Pittman, M., Choiniere, J., Hone, D.W.E., Upchurch, P., Tan, Q.-W., Xiao, D., and Tan, L. 2011a. The first known monodactyl non-avian dinosaur and the complex evolution of the alvarezsauroid hand. *Proceedings of National Academy of Sciences of the United States of America* 108: 2338-2342.
- Xu, X., Sullivan, C., Pittman, M., Choiniere, J., Hone, D.W.E., Upchurch, P., Tan, Q.-W., Xiao, D., and Tan, L. 2011b. Reply to Dyke and Naish: European alvarezsauroids do not change the picture. *Proceedings of the National Academy of Sciences of the United States of America*.
- Xu, X., Sullivan, C., Pittman, M., Choiniere, J., Hone, D.W.E., Upchurch, P., Tan, Q.-W., Xiao, D., and Tan, L. 2011c. Reply to Dyke and Naish: European alvarezsauroids do not change the picture. *Proceedings of the National Academy of Sciences of the United States of America* 108 (22): E148.
- Xu, X., Sullivan, C., Pittman, M., Choiniere, J., Hone, D.W.E., Upchurch, P., Tan, Q.-W., Xiao, D., Tan, L., and Han, F.L. 2011d. The first known monodactyl non-avian dinosaur and the complex evolution of the alvarezsauroid hand. *PNAS*: in press.
- Xu, X., Wang, D.Y., Sullivan, C., Hone, D., Han, F.L., Yan, R.-H., and Du, F.-M. 2010. A basal parvicursorine (Theropoda: Alvarezsauridae) from the Upper Cretaceous of China. *Zootaxa* 2413: 1-19.
- Zhou, Z.H. 1995. Is *Mononykus* a bird? *Auk* 112: 958-963.

[Figure legends]

Fig. 1. *Linhenykus monodactylus* holotype (IVPP V17608). Skeletal silhouette showing preserved bones (missing portions shown in grey).

Fig. 2. Cervical vertebrae of *Linhenykus monodactylus* holotype (IVPP V17608). Two posterior cervical vertebrae in right lateral (A), left lateral (B), ventral (C), and dorsal (D) views.

Abbreviations: dr, diapophyseal ridge; ep, epipophysis; pf, pneumatic foramen; pop, postzygaphophysis; pp, parapophysis; prp, prezygapophysis; vg, ventral groove; vk, ventral keel. Scale bar 5 mm.

Fig. 3. Dorsal vertebrae of *Linhenykus monodactylus* holotype (IVPP V17608). Middle dorsal vertebra in left lateral (A1), right lateral (A2), posterior (A3), ventral (A4), and dorsal (A5) views; two posterior dorsal vertebrae in lateral (B1) and ventral (B2) views. Abbreviations: con, condyle; di, diapophysis; ns, neural spine; pf, pneumatic foramen; pop, postzygaphophysis; pp, parapophysis; prp, prezygapophysis; vk, ventral keel. Scale bar 5 mm.

Fig. 4. Sacral vertebrae of *Linhenykus monodactylus* holotype (IVPP V17608). Presumed fourth and fifth last sacral vertebrae in left lateral (A1), right lateral (A2), ventral (A3), and dorsal (A4) views; presumed third and fourth last sacral vertebrae in right lateral (B1), left lateral (B2), and dorsal (B3) view; presumed second last sacral vertebra in right lateral (C1), anterior (C2), posterior (C3), and ventral (C4) views. Scale bar 5 mm.

Fig. 5. Caudal vertebrae 1-3 of *Linhenykus monodactylus* holotype (IVPP V17608). Caudal vertebra 1 in left lateral (A1) and right lateral (A2) views; caudal vertebrae 2 and 3 in anterior (B1), left lateral (B2), right lateral (B3), ventral (B4), and dorsal (B5) views. Abbreviations: con, condyle; nc, neural canal; ns, neural spine; pop, postzygaphophysis; prp, prezygapophysis; vk, ventral keel. Scale bar 5 mm.

Fig. 6. Caudal vertebrae 4-13 of *Linhenykus monodactylus* holotype (IVPP V17608). Caudal vertebrae 4-6 in left lateral (A1), right lateral (A2), ventral (A3), and dorsal (A4) views; caudal vertebra 7 in ventrolateral (B1), dorsolateral (B2), ventral (B3), and posterior (B4) views; caudal



vertebrae 8 and 9 in left lateral (C1), right lateral (C2), ventral (C3), and dorsal (C4) view; caudal vertebrae 10-12 in right lateral (D1), left lateral (D2), and ventral (D3) views; caudal vertebra 13 in right lateral (E1), left lateral (E2), ventral (E3), anterior (E4), and posterior (E5) views. Scale bar 5 mm.

Fig. 7. Left scapulocoracoid and sternum of *Linhenykus monodactylus* holotype (IVPP V17608). Left scapulocoracoid in lateral (A) view; sternum in ventral (B1) and anterior (B2) views. Abbreviations: co, coracoid; g, groove; gl, glenoid lip; sk, sternal keel. Scale bar 5 mm.

Fig. 8. Right humerus and left ulna of *Linhenykus monodactylus* holotype (IVPP V17608). Right humerus in anterior (A1), posterior (A2), and medial (A3) views; ?left ulna in anterior (B1), lateral (B2), and posterior (B3) views. Scale bar 5 mm.

Fig. 9. Manus of *Linhenykus monodactylus* holotype (IVPP V17608). Right manus in dorsal (A1) and dorsolateral (A2) views; right main carpometacarpal element in dorsal (B1), ventral (B2), proximal (B3), medial (B4), lateral (B5), and distal (B6) views; left main carpometacarpal element in dorsal (C1), proximal (C2), and distal (C3) views; metacarpal III in lateral (D1) and medial (D2) views; right manual phalanx II-1 in ventral (E) view, left manual phalanx II-2 in lateral (F1), proximal (F2), and ventral (F3) views. Abbreviations: amf, accessory medial facet; cef, central facet; ef, extensor fossa; mc III, metacarpal III; mc III de, distal end of metacarpal; mf, medial facet; mr, medial ridge; no, notch; ph II-1, phalanx II-1; ra, radiale; vg, ventral groove. Scale bars 5 mm.

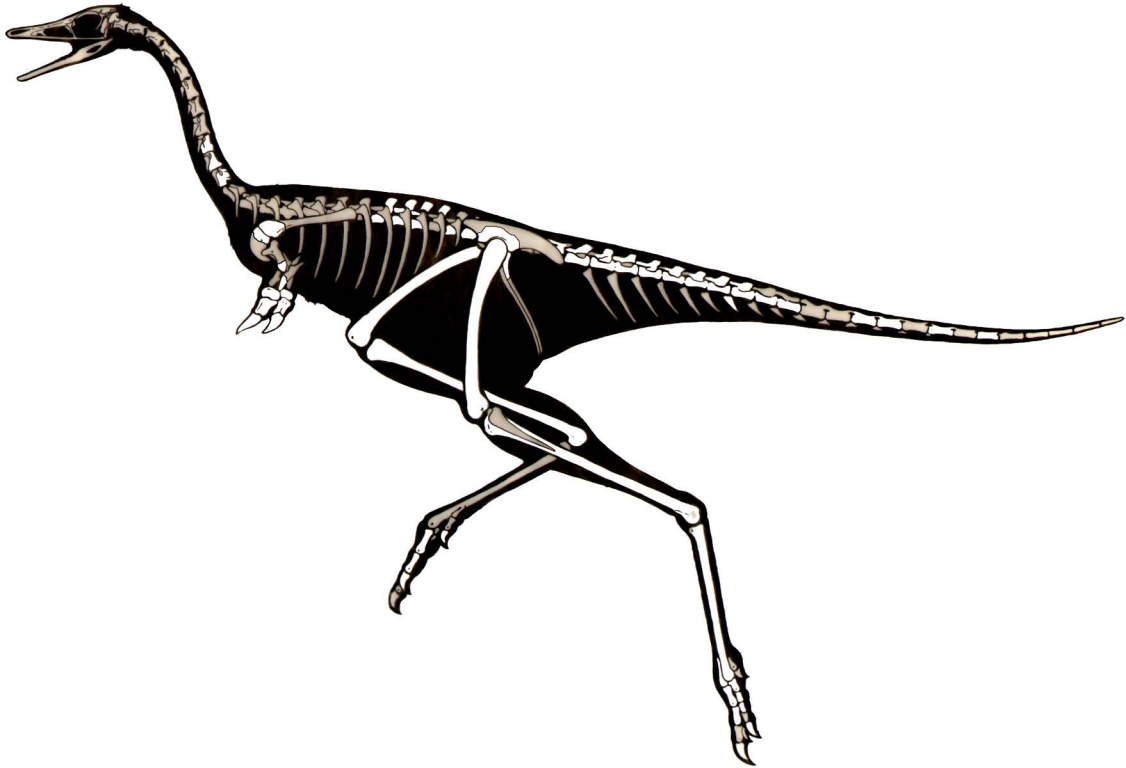
Fig. 10. Pelvic elements of *Linhenykus monodactylus* holotype (IVPP V17608). Left ilium in lateral (A1), dorsal (A2), and ventral (A3) views; left pubis in lateral (B1) view. Abbreviations: af, acetabular fossa; ppd, pubic peduncle; sc, supracetabular crest. Scale bar 5 mm.

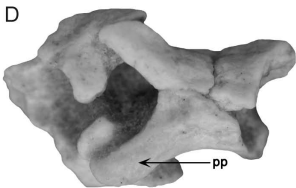
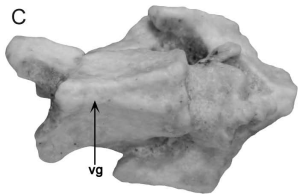
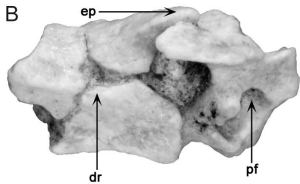
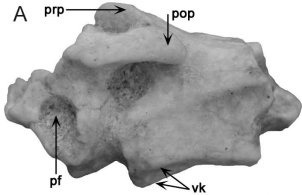
Fig. 11. Femora and tibiotarsi of *Linhenykus monodactylus* holotype (IVPP V17608). Right femur in proximal (A1), anterior (A2), posterior (A3), lateral (A4), medial (A5), and distal (A6) views; Left femur in anterior (B1), posterior (B2), and lateral (B3) views; left tibiotarsus in anterior (C1), posterior (C2), medial (C3), and lateral (C4) views; right tibiotarsus in anterior (D1), posterior (D2), and medial (D3) views; E1, left astragalus in anterior view. Abbreviations: ap, ascending process; fc,

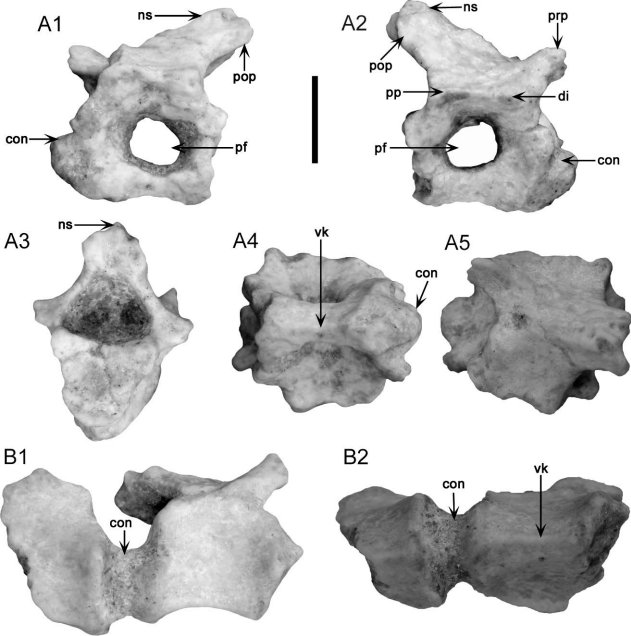
fibular crest; fh, femoral head; lc, lateral condyle; mc, medial condyle; pf, pneumatic foramen.  
Scale bar 10 mm.

Fig. 12. Pes of *Linhenykus monodactylus* holotype (IVPP V17608). Left metatarsus in dorsal (A1), ventral (A2), medial (A3), and lateral (A4) views; left pedal phalanges I-1 and I-2 in right (B1) and left (B2) lateral views; ?right pedal phalanges II-1, II-2, and II-3 in lateral (C1), dorsal (C2), ventral (C3) views; ?left pedal phalanges IV-3 , IV-4 , and IV-5 in dorsal (D1), ventral (D2), and lateral (D3) views; ?right pedal phalanx IV-4 in proximal (E1), dorsal (E2), lateral (E3), medial (E4), and distal (E5) views; F1, ?left pedal phalanges III-3 and III-4 in lateral view. Abbreviations: mr, medial ridge; mt II, metatarsal II; mt IV, metatarsal IV; no, notch; p II-1, pedal phalanx II-1; p II-2, pedal phalanx II-2; p IV-1, pedal phalanx IV-1. Scale bars 5 mm.

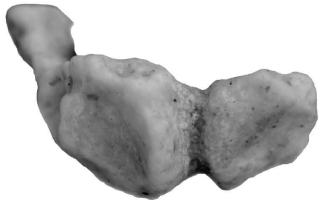
Fig. 13. The two trees produced by resolving the basal trichotomy in the alvarezsaurid clade (see text for details). Tree 1 is used in data set 1 and Tree 2 in data set 2 (see Appendix 2). The geographic regions occupied by each terminal taxon are shown: A, Asia; N, North America; S, South America



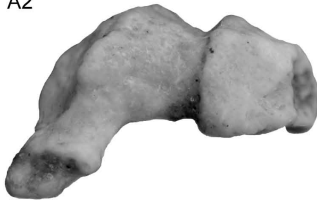




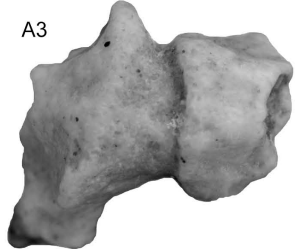
A1



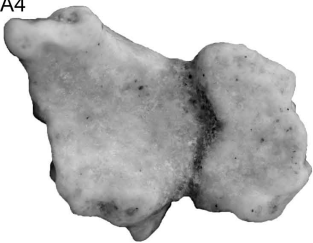
A2



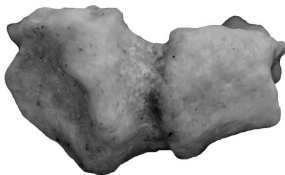
A3



A4



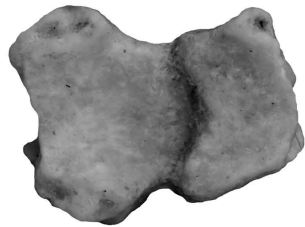
B1



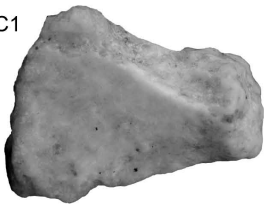
B2



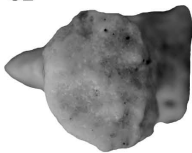
B3



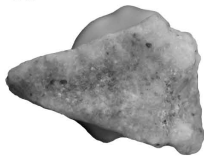
C1



C2



C3



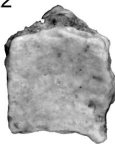
C4



A1

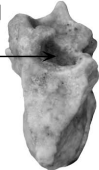


A2



B1

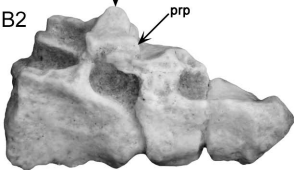
nc



B2

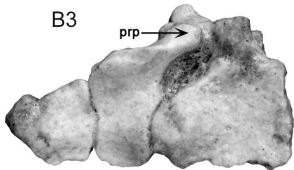
ns

prp



B3

prp



B4

vk

vk



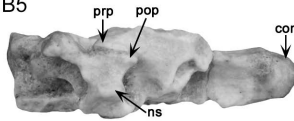
B5

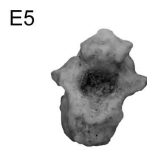
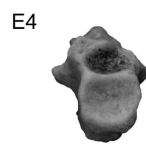
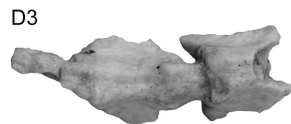
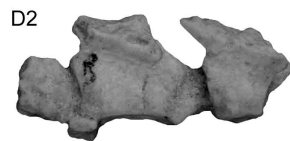
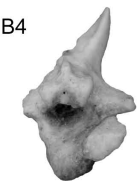
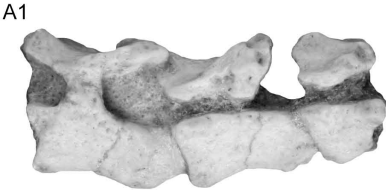
prp

pop

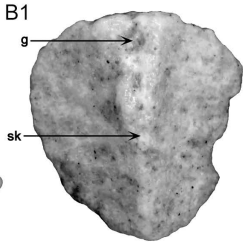
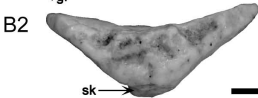
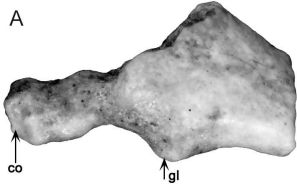
con

ns









A1



A2



A3



B1

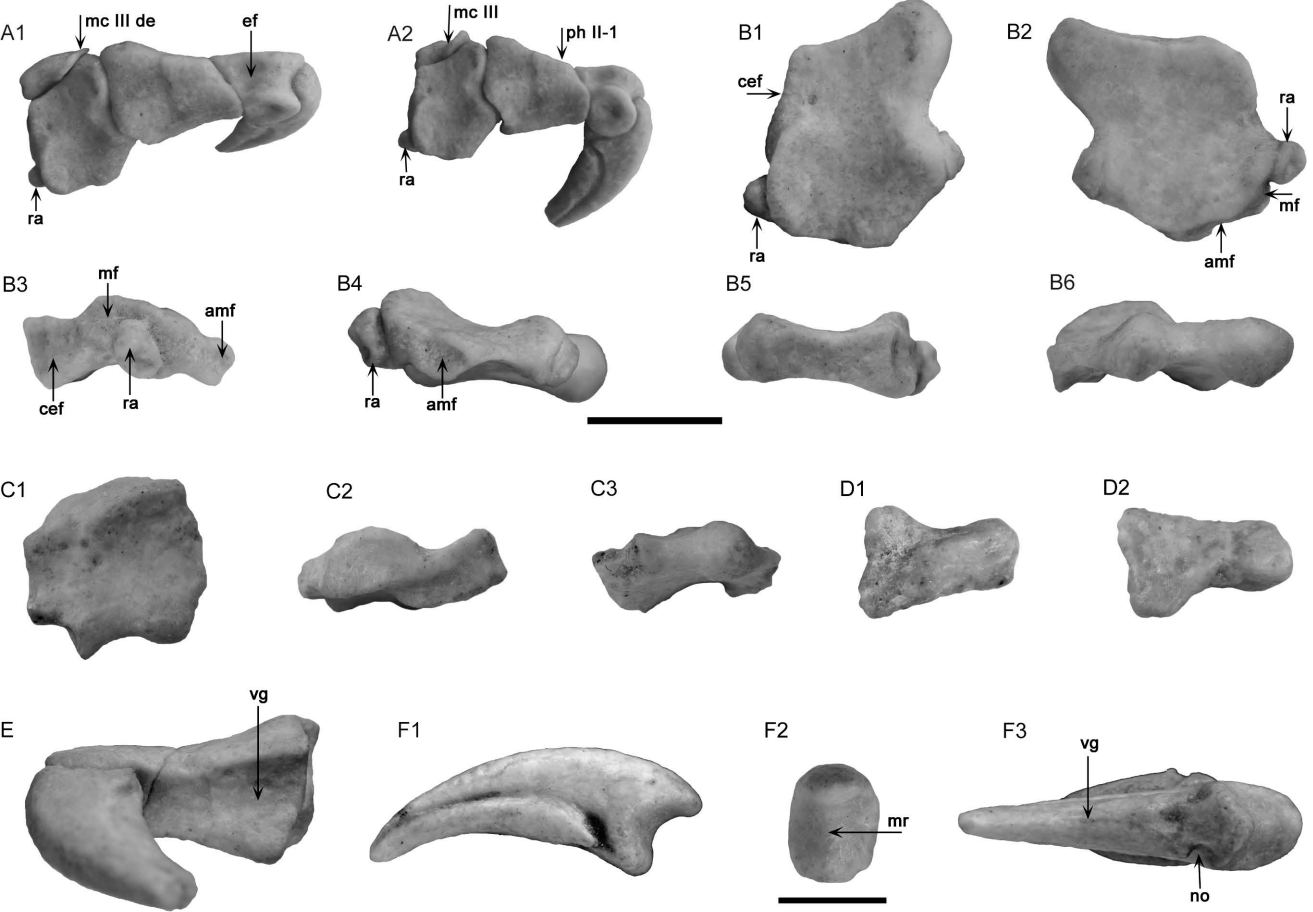


B2

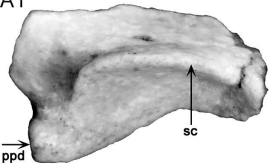


B3

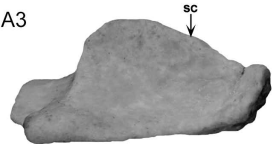




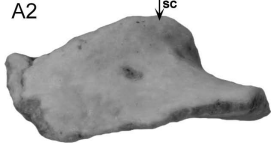
A1



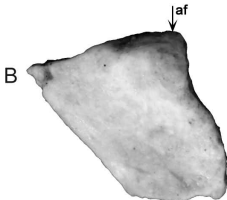
A3



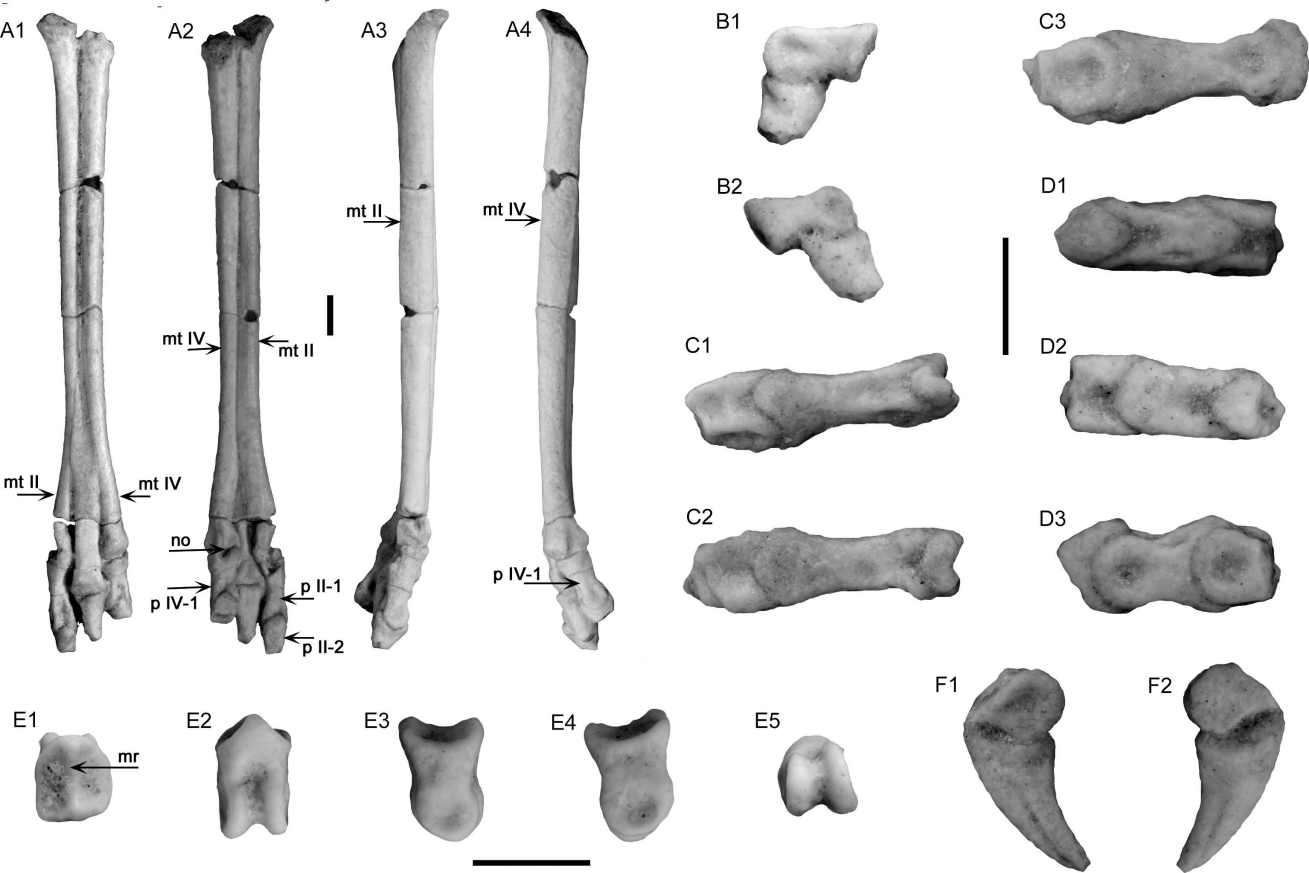
A2



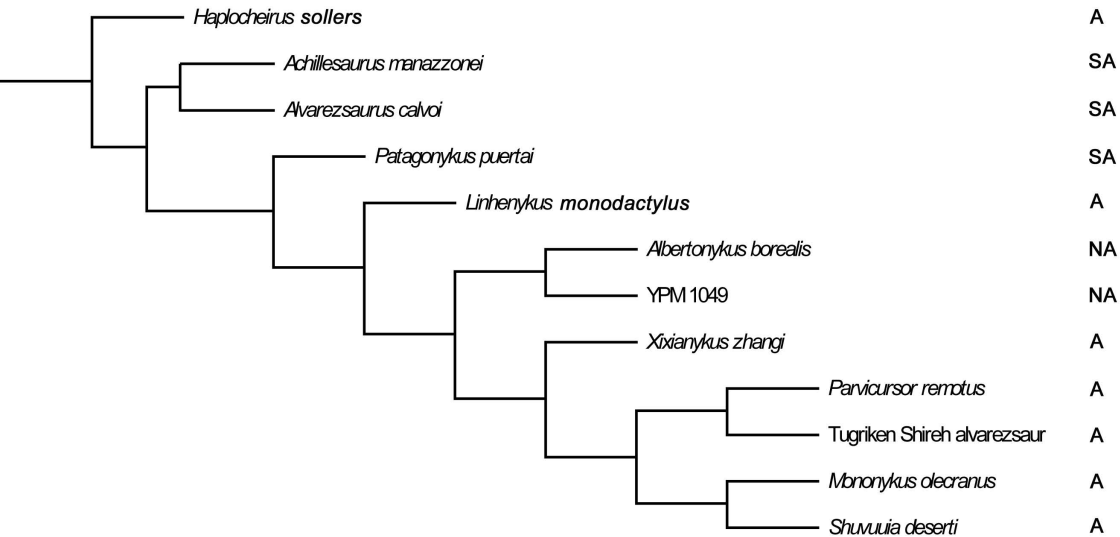
B







A



B

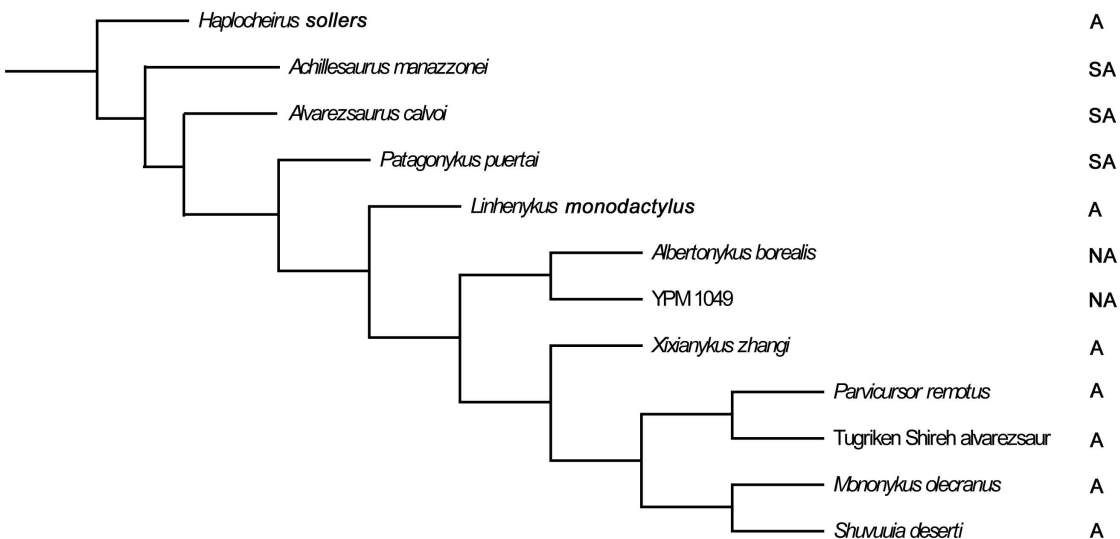


Table 1. Summary of the results of the Treefitter analyses of data sets 1 and 2 (see Appendix 2).  
Abbreviations: DC, default event costs; MC, maximum codivergence event costs; OAC, optimal area cladogram; rec. cost, total cost of the most parsimonious biogeographic reconstruction.

Data set	Cost regime	OAC	Rec. cost	<i>p</i> -value
1	DC	(S(A,N)), (N(A,S))	4	0.0054- 0.091
1	MC	(S(A,N)), (A(N,S))	-2	0.997-0.999
2	DC	(S(A,N)), (N(A,S))	8	0.0077- 0.0178
2	MC	(S(A,N)), (A(N,S))	-4	0.999



Table 2. Summary of event frequencies reconstructed using Treefitter. Abbreviations: DC, default costs; MC, maximum codivergence costs; F. Disp., dispersal frequency; F. Ext., extinction frequency; F. Symp., sympatry frequency; F. Vic., vicariance frequency. Only statistically significant *p*-values are shown. ‘+’ and ‘-’ indicate that the frequency of the event in the real data is greater than or less than expected from random data, respectively.

Data set	Cost regime	F. Vic.	F. Symp.	F. Ext.	F. Disp.
1	DC	1-2	8-9 ( $p = 0.0062$ - $0.0077$ ) +	0-4	0-2
1	MC	2	6-9	0-3	0-3
2	DC	2-4	16-17 ( $p = 0.0016$ - $0.0025$ ) +	0.6 ( $p = 0.0258$ ) -	1-4
2	MC	4 ( $p = 0.0068$ - $0.132$ )-	11-18 ( $p = 0.0122$ - $0.75$ ) +	0-10 ( $p = 0.0466$ - $0.35$ )-	0-7

## Appendix 1

See Longrich and Currie (2009) for the character list.

Unambiguous synapomorphies for the Alvarezsauroidea: cervical epipophyses reduced or absent (character state 6.1), coracoid with elongate ventrolateral process (character state 25.1), humeral internal tuberosity hypertrophied and proximally projecting (character state 29.1), humeral ectepicondyle hypertrophied and distally positioned (character state 31.1), distal articular surface of ulna bulbous and trochlear (character state 33.1), olecranon process of ulna hypertrophied (character state 34.1), manual digit II subequal to humerus in diameter (character state 40.1), manual phalanx II-1 flattened and bearing a prominent ventral sulcus (character state 40.1), postacetabular process of ilium longer than preacetabular process (character state 50.1), and femoral lateral condyle conical and distally projecting (character state 61.1);

Unambiguous synapomorphies for Alvarezsauridae: cervical centra bearing deep lateral depressions (character state 8.1), posterior sacral vertebrae bearing a large ventral keel (character state 19.1), caudal vertebrae procoelous (character state 21.1), coracoidal biceps tubercle reduced or absent (character state 26.1), manual ungual II flexor tubercle reduced to a low keel (character state 44.1), proximal articular surface of manual ungual II at least as broad as tall (character state 46.1), pubic peduncle of ilium anteroposteriorly reduced (character state 48.1), medial shelf of brevis fossa reduced to a low ridge (character state 53.1), and pedal digit III more slender than either digit II or IV (character state 73.1);

Unambiguous synapomorphies for Parvicursorinae: dorsal vertebrae opisthocoelous (character state 10.1), dorsal vertebrae without hyposphene-hypantrum articulations (character state 12.1), parapophyses of dorsal vertebrae elevated to the level of the diapophyses (character state 13.1), dorsal infradiapophyseal fossa and infraprezygapophyseal fossa invisible in lateral view (character state 15.1), posterior sacral bearing a hypertrophied ventral keel (character state 19.2), anterior caudals with transverse processes anteriorly positioned on centrum (character state 22.1), metacarpal II with prominent tuberosity ('extensor process') on medial surface (character state 39.1), ventral surface of manual ungual II bearing axial groove (character state 43.1), manual ungual II without well-developed flexor tubercle (character state 44.2), ascending process of astragalus restricted and failing to cover medial surface of tibia (character state 66.1), shaft of metatarsal III triangular in section and proximally reduced (character state 68.1), and distal end of tibia with lateral malleolus anteroposteriorly expanded (character state 77.1).

## Appendix 2

To replicate the Treefitter analyses, the reader should copy the text between quotation marks into a text only (‘.txt’) document and then follow the instructions in the manual that accompanies Treefitter 2.0b (Ronquist 1998)

### Data set 1

‘Ptree alvarezsaur1

*(Haplocheirus, ((Achillesaurus, Alvarezsaurus), (Patagonykus, (Linhenykus, ((Albertonykus, YPM1049), (Xixianykus, ((Mononykus, Shuvuuia), (Parvicursor, TugrikenShirehalvrezsaur))))))));*

Range alvarezsaur1 *Haplocheirus:A, Achillesaurus:S, Alvarezsaurus:S, Patagonykus:S, Linhenykus:A, Albertonykus:N, YPM1049:N, Xixianykus:A, Mononykus:A, Shuvuuia:A, Parvicursor:A, TugrikenShirehalvrezsaur:A;*’

### Data set 2

‘Ptree alvarezsaur2

*(Haplocheirus, (Achillesaurus, (Alvarezsaurus, (Patagonykus, (Linhenykus, ((Albertonykus, YPM1049), (Xixianykus, ((Mononykus, Shuvuuia), (Parvicursor, TugrikenShirehalvrezsaur))))))));*

Range alvarezsaur2 *Haplocheirus:A, Achillesaurus:S, Alvarezsaurus:S, Patagonykus:S, Linhenykus:A, Albertonykus:N, YPM1049:N, Xixianykus:A, Mononykus:A, Shuvuuia:A, Parvicursor:A, TugrikenShirehalvrezsaur:A;*’